제 17회 응집물리 여름학교

광분광학 (2)

대구경북과학기술원 (DGIST) 화학물리학과

김소연

Contents

Spectroscopic ellipsometry

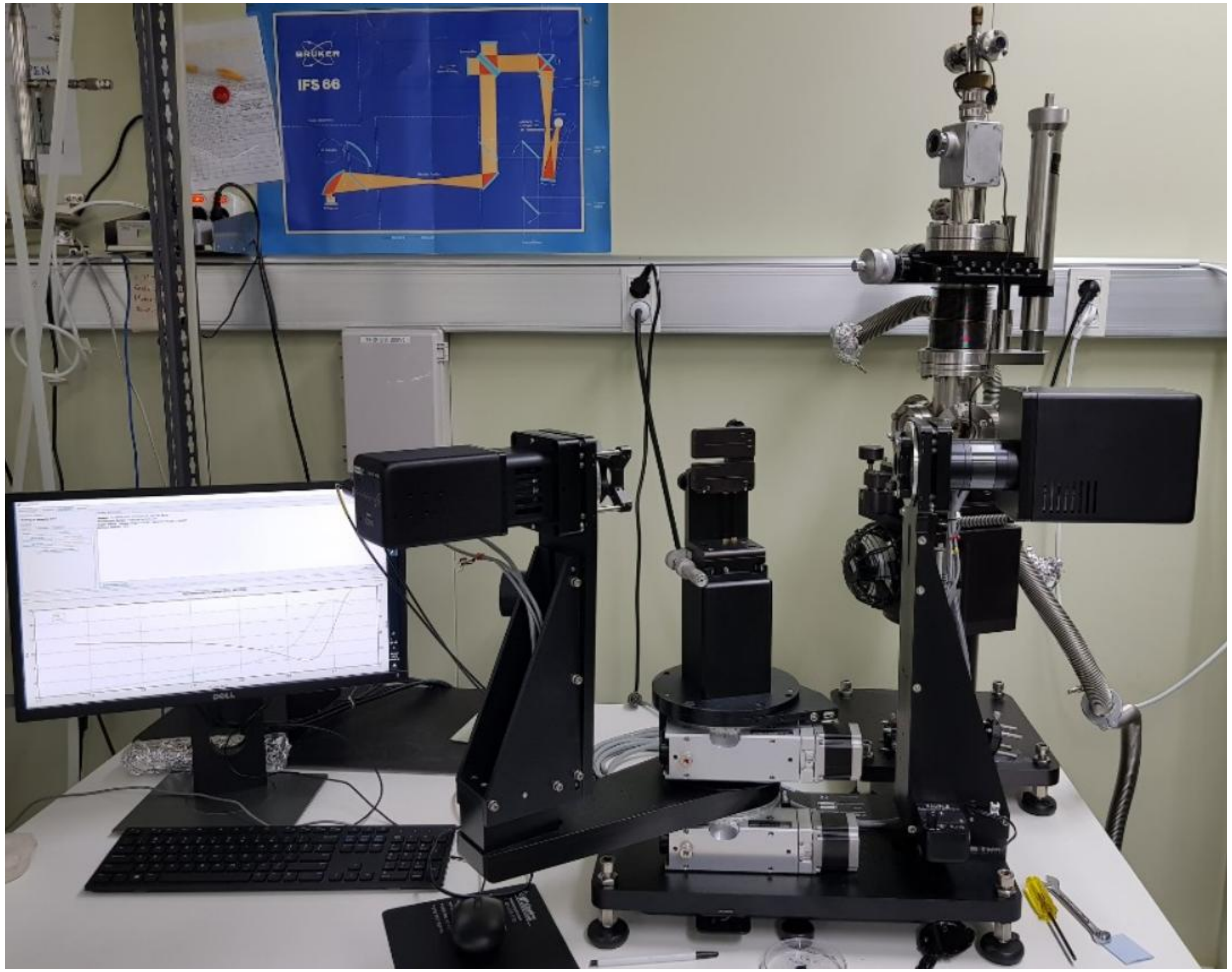

***In-situ* ellipsometer**
0.74 meV – 6.5 eV (UV/vis)

IR ellipsometer
60 meV – 0.5 eV (IR)

- 타원편광분광기
- 투과율, 반사율 측정 가능
- $Re^{i\theta}$ 의 R, θ 동시 측정
  $\Rightarrow$ Kramers-Kronig relation 불필요

- Fresnel equation 모델링을 통해
  매우 얇은 박막 (~10 nm) 시료 두께 측정
- 증착과정에서 In-situ 측정 가능

Polarization of light

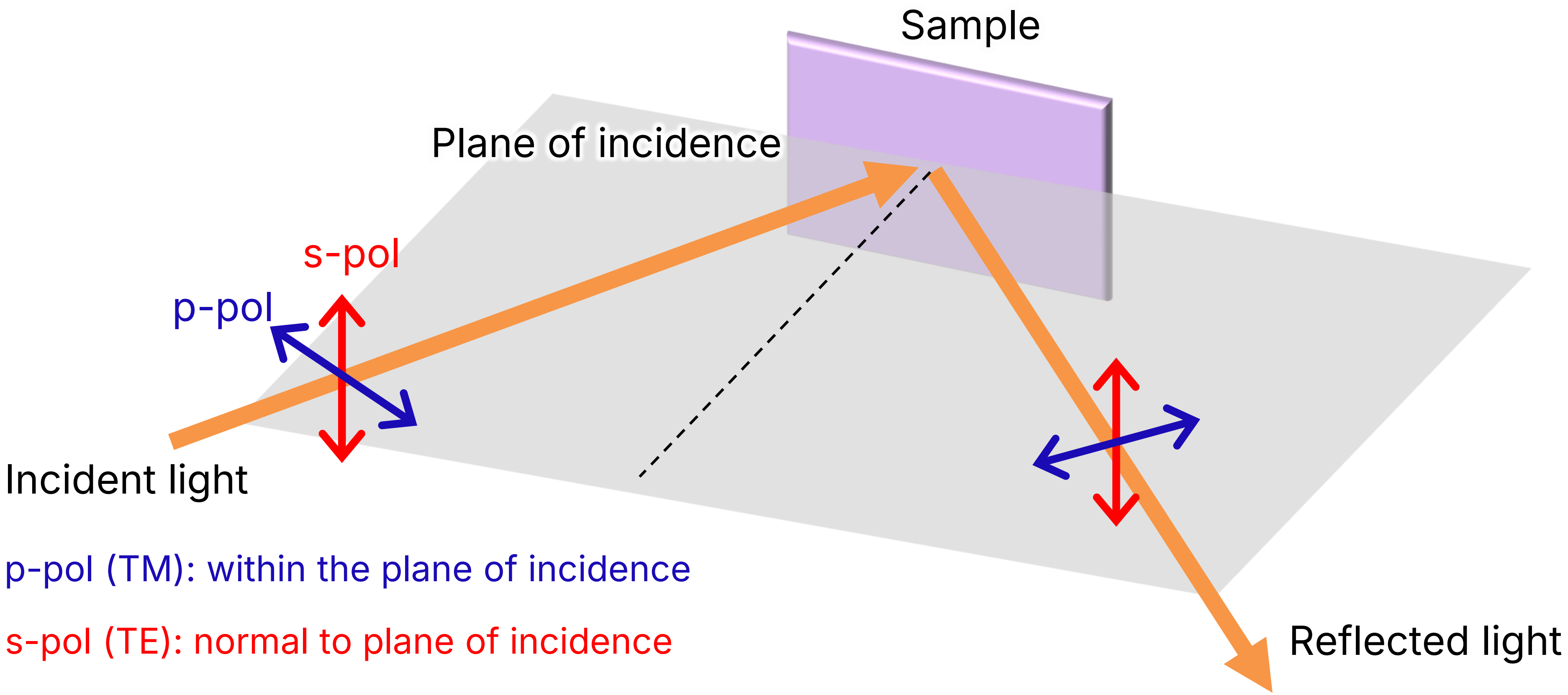

p-pol (TM): within the plane of incidence

s-pol (TE): normal to plane of incidence

German: senkrecht (perpendicular/normal; ⊥); parallel (parallel; ||)

- Polarized light:
  The electric field of waves are oriented in specific direction.

Polarization of light

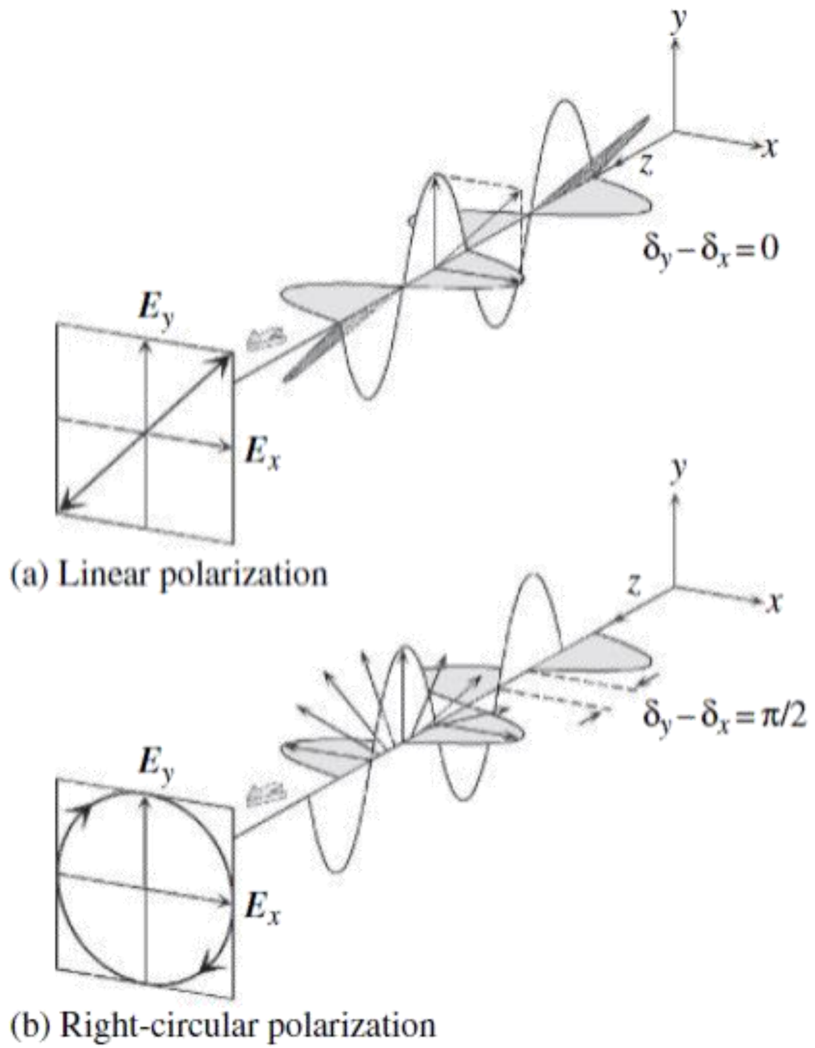

- Polarized light:
  The electric field of waves are oriented in specific direction.

- Photon is a spin-1 boson ⇒ helicity (LHC, RHC) for m_s = ±1
  Note. m_s = 0 (longitudinal) state is forbidden (zero mass)

- Linear polarized light is a linear combinations of circularly polarized light.

$$\boldsymbol{E}(z,t)=\boldsymbol{E}_x(z,t)+\boldsymbol{E}_y(z,t)$$
$$=\{E_{x0}\exp[i(\omega t-Kz+\delta_x)]\}\boldsymbol{x}+\{E_{y0}\exp[i(\omega t-Kz+\delta_y)]\}\boldsymbol{y}$$

$$E_{\mathrm{R}}=\frac{1}{\sqrt{2}}\begin{bmatrix}1\\ \mathrm{i}\end{bmatrix}\quad E_{\mathrm{L}}=\frac{1}{\sqrt{2}}\begin{bmatrix}1\\ -\mathrm{i}\end{bmatrix}$$

Jones vector

$$E_{\mathrm{linear},x}=\begin{bmatrix}1\\0\end{bmatrix}\quad E_{\mathrm{linear},y}=\begin{bmatrix}0\\1\end{bmatrix}$$

Elliptical polarization

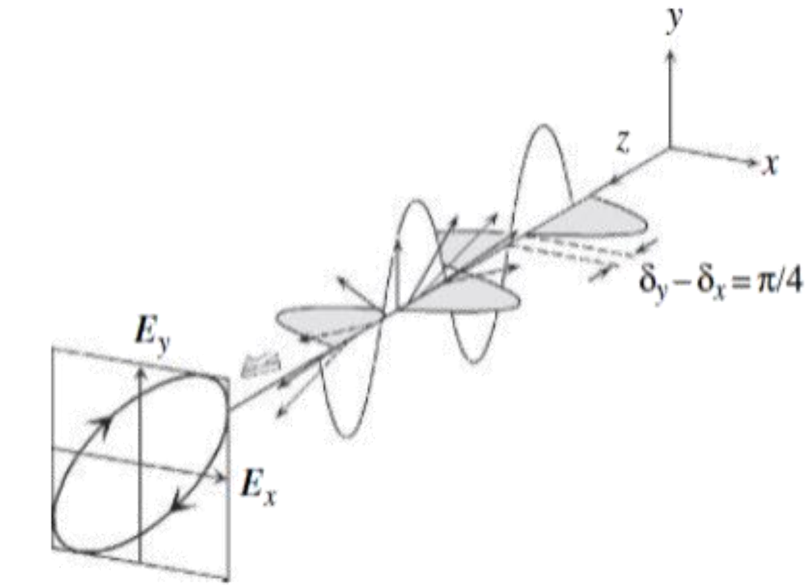

(c) Elliptical polarization

- Linear polarized light is a linear combinations of circularly polarized light.
- Other polarizations (except δ = 0 (mod 2π) & ±π/2) are all elliptical polarization.

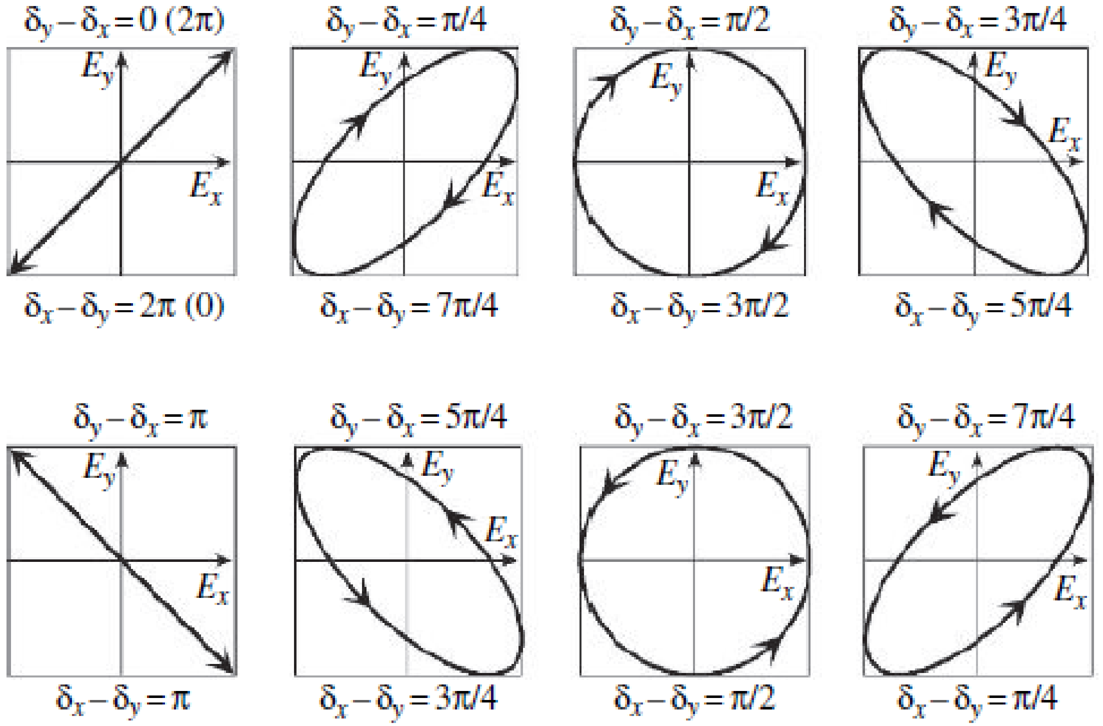

Fresnel formula

Fresnel's equation for normal incidence

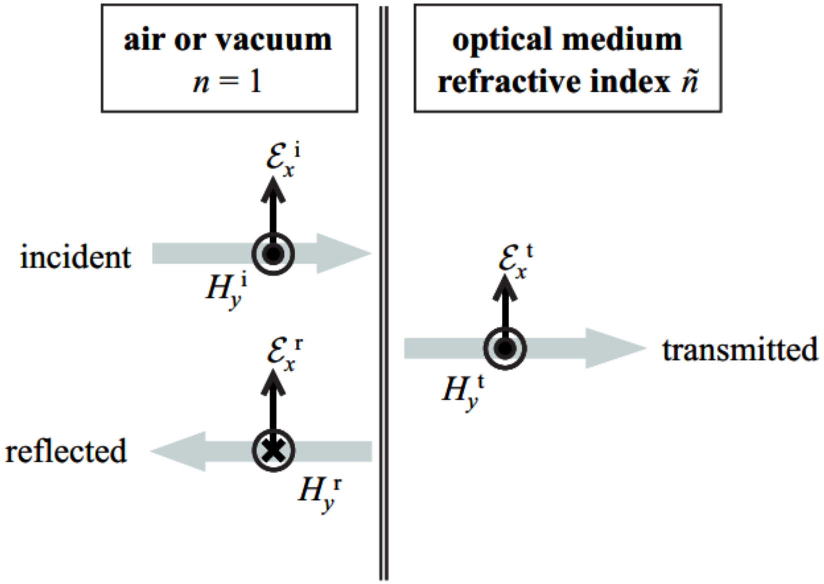

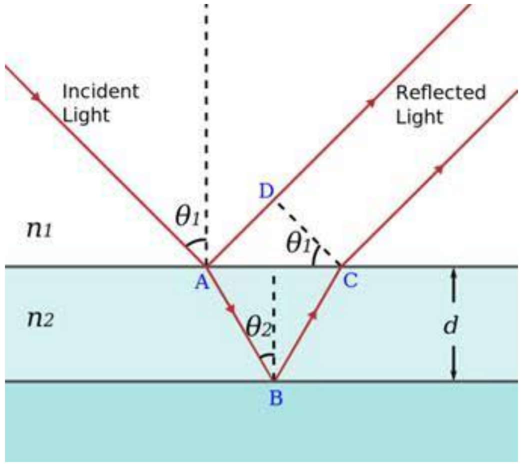

Thin film (film + substrate)

Maxwell's equations

+

Boundary conditions

The tangential components of the electric and magnetic fields are continuous.

$$\mathcal{E}_x^{\mathrm{i}} + \mathcal{E}_x^{\mathrm{r}} = \mathcal{E}_x^{\mathrm{t}}$$

$$H_y^{\mathrm{i}} - H_y^{\mathrm{r}} = H_y^{\mathrm{t}}$$

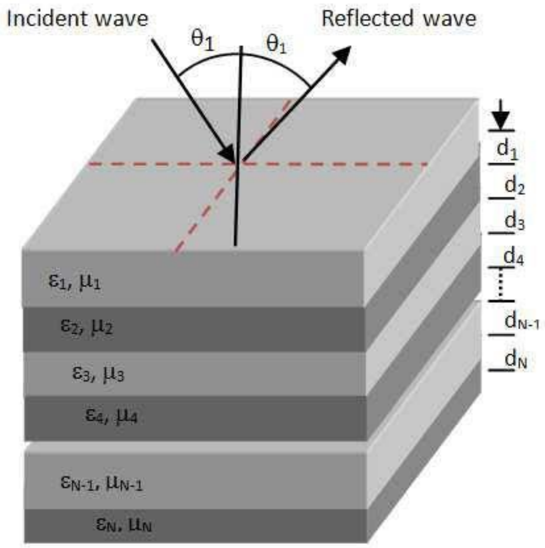

Superlattice thin film (alternating/repeated heterostructure + substrate)

Jones matrix

Jones vector

Note. Unpolarized (depolarized) light cannot be expressed

$$E(z,t) = E_x(z,t) + E_y(z,t)$$
$$= \{E_{x0}\exp[i(\omega t - Kz + \delta_x)]\}x + \{E_{y0}\exp[i(\omega t - Kz + \delta_y)]\}y$$

$$E_R = \frac{1}{\sqrt{2}}\begin{bmatrix}1\\ i\end{bmatrix} \quad E_L = \frac{1}{\sqrt{2}}\begin{bmatrix}1\\ -i\end{bmatrix}$$

$$E_{\mathrm{linear},x} = \begin{bmatrix}1\\ 0\end{bmatrix} \quad E_{\mathrm{linear},y} = \begin{bmatrix}0\\ 1\end{bmatrix}$$

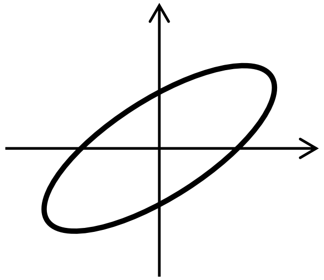

$$\begin{bmatrix}\sin\psi\exp(i\Delta)\\ \cos\psi\end{bmatrix}$$

- Jones matrix is a matrix representation that allows the mathematical description of optical measurements.
- The variation in polarized light from many optical elements can be applied easily in matrix calculation.
- Arbitrary polarized can be represented with two parameter: Ψ and Δ

Jones matrix for various optics

Optical element	Jones matrix
Polarizer[a] (Analyzer) $P(A)$	$\begin{bmatrix}1 & 0\\ 0 & 0\end{bmatrix}$
Compensator[b] (Retarder) C	$\begin{bmatrix}1 & 0\\ 0 & \exp(-i\delta)\end{bmatrix}$
Photoelastic modulator[c] M	$\begin{bmatrix}1 & 0\\ 0 & \exp(i\delta)\end{bmatrix}$
Coordinate rotation[d] $R(\alpha)$	$\begin{bmatrix}\cos\alpha & \sin\alpha\\ -\sin\alpha & \cos\alpha\end{bmatrix}$
Sample[e] S	$\begin{bmatrix}\sin\psi\exp(i\Delta) & 0\\ 0 & \cos\psi\end{bmatrix}$

Jones matrix

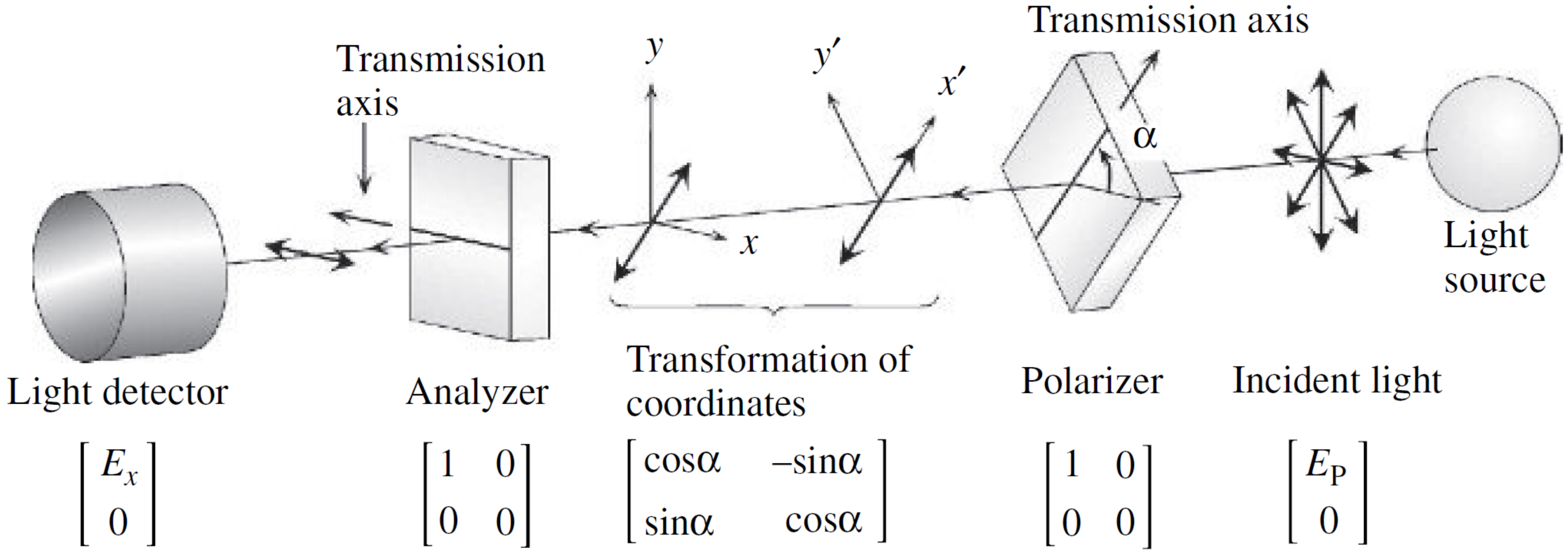

- Jones matrix is a matrix representation that allows the mathematical description of optical measurements.
- The variation in polarized light from many optical elements can be applied easily in matrix calculation.
- Arbitrary polarized can be represented with two parameter: Ψ and Δ

Jones matrix for various optics

Optical element	Jones matrix
Polarizer[a] (Analyzer) *P(A)*	$\begin{bmatrix} 1 & 0 \\ 0 & 0 \end{bmatrix}$
Compensator[b] (Retarder) *C*	$\begin{bmatrix} 1 & 0 \\ 0 & \exp(-i\delta) \end{bmatrix}$
Photoelastic modulator[c] *M*	$\begin{bmatrix} 1 & 0 \\ 0 & \exp(i\delta) \end{bmatrix}$
Coordinate rotation[d] *R(α)*	$\begin{bmatrix} \cos\alpha & \sin\alpha \\ -\sin\alpha & \cos\alpha \end{bmatrix}$
Sample[e] *S*	$\begin{bmatrix} \sin\psi\exp(i\Delta) & 0 \\ 0 & \cos\psi \end{bmatrix}$

Stokes parameters (Stokes vector)

- Stokes parameter allows the description of unpolarized (depolarized) and partial polarized light.
  ⇒ Covers ALL types of polarization

$$S_0 = I_x + I_y$$

Total light intensity

$$\left.\begin{aligned} S_1 &= I_x - I_y \\ S_2 &= I_{+45^\circ} - I_{-45^\circ} \\ S_3 &= I_{\mathrm{R}} - I_{\mathrm{L}} \end{aligned}\right\}$$

The relative intensity difference for each pol.

S_1 > 0: polarized towards the ***x***-direction

S_3 < 0: polarized towards the LHC ⟳

Table 3.1 Representations of the states of polarization by the Jones and Stokes vectors

Polarization	Polarization state	Jones vector	Stokes vector
Linear polarization parallel to x axis	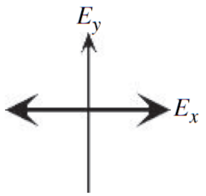	$\begin{bmatrix}1\\0\end{bmatrix}$	$\begin{bmatrix}1\\1\\0\\0\end{bmatrix}$
Linear polarization parallel to y axis	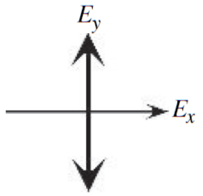	$\begin{bmatrix}0\\1\end{bmatrix}$	$\begin{bmatrix}1\\-1\\0\\0\end{bmatrix}$
Linear polarization oriented at 45°	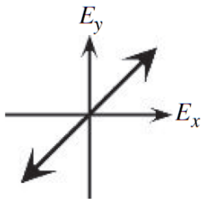	$\frac{1}{\sqrt{2}}\begin{bmatrix}1\\1\end{bmatrix}$	$\begin{bmatrix}1\\0\\1\\0\end{bmatrix}$

Stokes parameters (Stokes vector)

- Stokes parameter allows the description of unpolarized (depolarized) and partial polarized light.
  ⇒ Covers ALL types of polarization

$$S_0 = I_x + I_y$$

Total light intensity

$$S_1 = I_x - I_y$$

$$S_2 = I_{+45^\circ} - I_{-45^\circ}$$

$$S_3 = I_R - I_L$$

The relative intensity difference for each pol. (S_1, S_2, S_3)

S_1 > 0: polarized towards the ***x***-direction

S_3 < 0: polarized towards the LHC ⟳

Table 3.1 Representations of the states of polarization by the Jones and Stokes vectors

Polarization	Polarization state	Jones vector	Stokes vector
Right-circular polarization	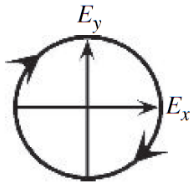	$\frac{1}{\sqrt{2}}\begin{bmatrix}1\\ \mathrm{i}\end{bmatrix}$	$\begin{bmatrix}1\\0\\0\\1\end{bmatrix}$
Left-circular polarization	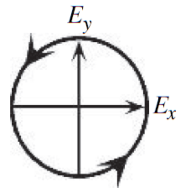	$\frac{1}{\sqrt{2}}\begin{bmatrix}1\\ -\mathrm{i}\end{bmatrix}$	$\begin{bmatrix}1\\0\\0\\-1\end{bmatrix}$
Elliptical polarization	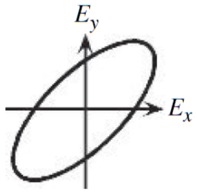	$\begin{bmatrix}\sin\psi\exp(\mathrm{i}\Delta)\\ \cos\psi\end{bmatrix}$	$\begin{bmatrix}1\\ -\cos 2\psi\\ \sin 2\psi\cos\Delta\\ -\sin 2\psi\sin\Delta\end{bmatrix}$
Natural light (unpolarized light)			$\begin{bmatrix}1\\0\\0\\0\end{bmatrix}$

For derivation from electric field, see Fujiwara et al.

Stokes parameters (Stokes vector)

- Stokes parameter allows the description of unpolarized (depolarized) and partial polarized light.
  ⇒ Covers ALL types of polarization

$$S_0 = I_x + I_y$$ Total light intensity

$$S_1 = I_x - I_y$$
$$S_2 = I_{+45^\circ} - I_{-45^\circ}$$
$$S_3 = I_R - I_L$$

The relative intensity difference for each pol.

$S_1 > 0$: polarized towards the ***x***-direction

$S_3 < 0$: polarized towards the LHC ⟳

Ellipticity/Rotation **Amplitude/phase ratio**

(a) (ε, θ) coordinate system (b) (ψ, Δ) coordinate system

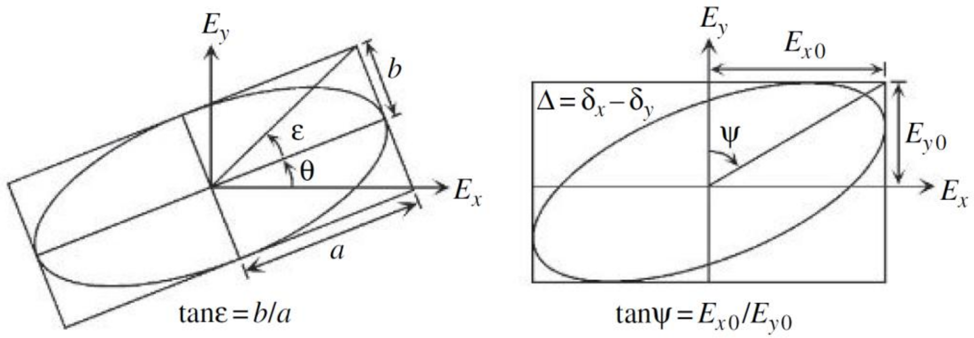

	S_0	S_1	S_2	S_3
Light intensity	$I_x + I_y$	$I_x - I_y$	$I_{+45^\circ} - I_{-45^\circ}$	$I_R - I_L$
(ε, θ) system	1	$\cos 2\varepsilon \cos 2\theta$	$\cos 2\varepsilon \sin 2\theta$	$\sin 2\varepsilon$
(ψ, Δ) system	1	$-\cos 2\psi$	$\sin 2\psi \cos \Delta$	$-\sin 2\psi \sin \Delta$

- To specify an arbitrary polarized light, two parameters are required: (Ψ, Δ) or (ε, θ)
  ⇒ Fresnel equation
  ⇒ Complex optical constants $(n + i\kappa)$, or $(\varepsilon_1 + i\varepsilon_2)$, or $(\sigma_1 + i\sigma_2)$, or $(Re^{i\theta})$, ...

Mueller matrix

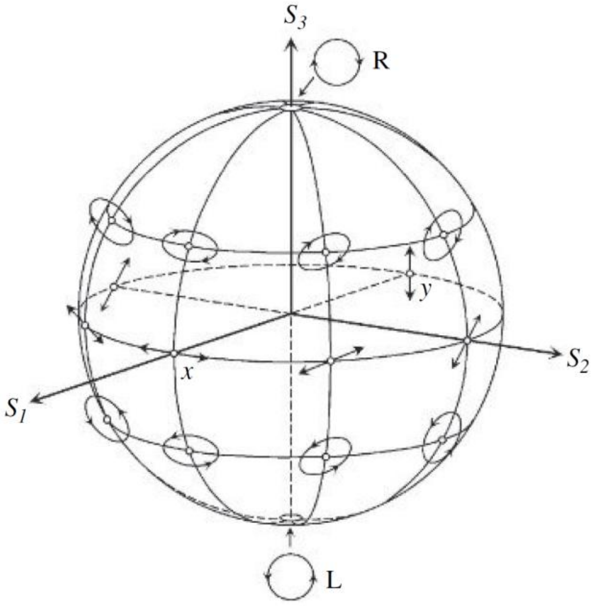

Poincare sphere of S_1, S_2, and S_1 can represent all polarization states

- The variation in polarized light from many optical elements can be applied easily in matrix calculation using Stokes vector and Mueller matrix.
- For highly anisotropic/birefringent samples or those with depolarized light, Mueller matrix should be measured.

Mueller matrix for various optics

Table 3.2 Jones and Mueller matrices for optical elements and coordinate rotation

Optical element	Jones matrix	Mueller matrix
Polarizer[a] (Analyzer) ***P(A)***	$\begin{bmatrix} 1 & 0 \\ 0 & 0 \end{bmatrix}$	$\frac{1}{2}\begin{bmatrix} 1 & 1 & 0 & 0 \\ 1 & 1 & 0 & 0 \\ 0 & 0 & 0 & 0 \\ 0 & 0 & 0 & 0 \end{bmatrix}$
Compensator[b] (Retarder) ***C***	$\begin{bmatrix} 1 & 0 \\ 0 & \exp(-i\delta) \end{bmatrix}$	$\begin{bmatrix} 1 & 0 & 0 & 0 \\ 0 & 1 & 0 & 0 \\ 0 & 0 & \cos\delta & \sin\delta \\ 0 & 0 & -\sin\delta & \cos\delta \end{bmatrix}$
Photoelastic modulator[c] ***M***	$\begin{bmatrix} 1 & 0 \\ 0 & \exp(i\delta) \end{bmatrix}$	$\begin{bmatrix} 1 & 0 & 0 & 0 \\ 0 & 1 & 0 & 0 \\ 0 & 0 & \cos\delta & -\sin\delta \\ 0 & 0 & \sin\delta & \cos\delta \end{bmatrix}$
Coordinate rotation[d] ***R***(α)	$\begin{bmatrix} \cos\alpha & \sin\alpha \\ -\sin\alpha & \cos\alpha \end{bmatrix}$	$\begin{bmatrix} 1 & 0 & 0 & 0 \\ 0 & \cos 2\alpha & \sin 2\alpha & 0 \\ 0 & -\sin 2\alpha & \cos 2\alpha & 0 \\ 0 & 0 & 0 & 1 \end{bmatrix}$
Sample[e] ***S***	$\begin{bmatrix} \sin\psi\exp(i\Delta) & 0 \\ 0 & \cos\psi \end{bmatrix}$	$A\begin{bmatrix} 1 & -\cos 2\psi & 0 & 0 \\ -\cos 2\psi & 1 & 0 & 0 \\ 0 & 0 & \sin 2\psi\cos\Delta & \sin 2\psi\sin\Delta \\ 0 & 0 & -\sin 2\psi\sin\Delta & \sin 2\psi\cos\Delta \end{bmatrix}$
Depolarizer ***D***		$\begin{bmatrix} 1 & 0 & 0 & 0 \\ 0 & 0 & 0 & 0 \\ 0 & 0 & 0 & 0 \\ 0 & 0 & 0 & 0 \end{bmatrix}$

[a] Transmission axis is parallel to the x axis
[b] fast axis is parallel to the x axis and δ is given by Eq. (3.3)
[c] δ is given by Eq. (3.4)
[d] coordinate rotation is counterclockwise (see Fig. 3.11)

Principles of spectroscopic ellipsometry

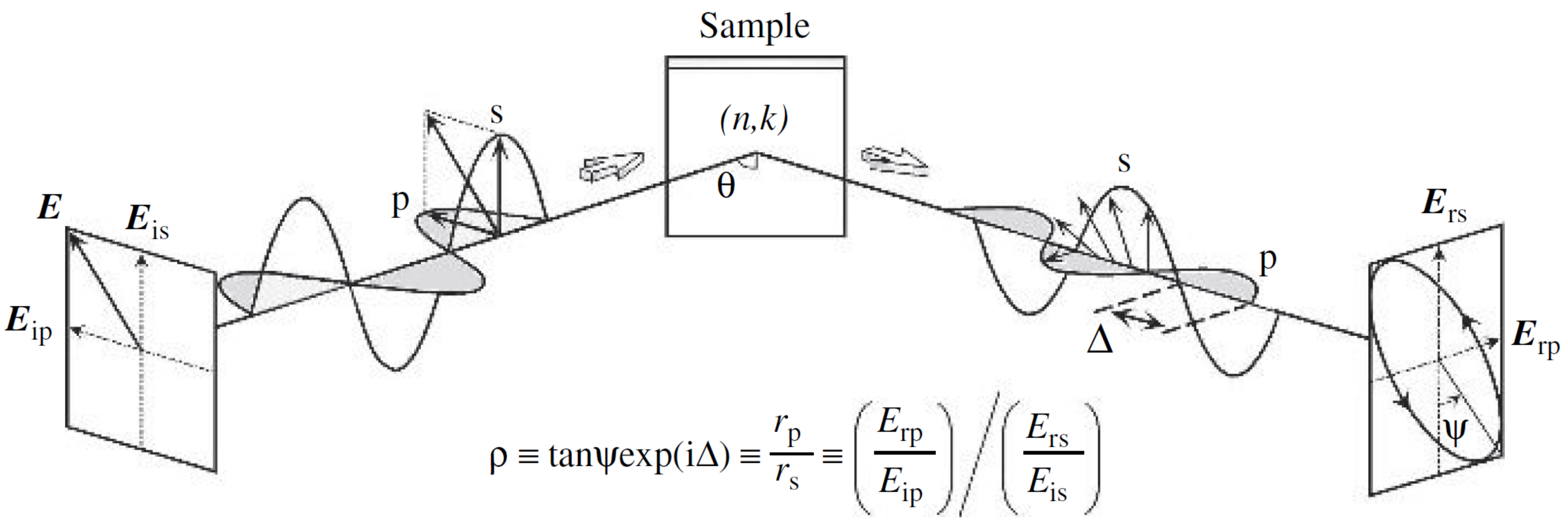

Figure 4.1 Measurement principle of ellipsometry.

Experimentally measured: ψ & Δ

$$\rho \equiv \tan\psi \exp(i\Delta) \equiv \frac{r_p}{r_s} \equiv \left(\frac{E_{rp}}{E_{ip}}\right) \Big/ \left(\frac{E_{rs}}{E_{is}}\right)$$

$$\tan\psi = |r_p|/|r_s| \quad \Delta = \delta_{rp} - \delta_{rs}$$

- To make the optical fitting more unique, the ψ & Δ are measured at several incidence angles (50°, 60°, 70°)
- Angles near the Brewster angle (~60°)⇒ to maximize the R_p and R_s difference
  $\theta_B(n) = \arctan(n)$; $\theta_B(1.3) \sim 52°$; $\theta_B(1.7) \sim 60°$; $\theta_B(2.0) \sim 63°$;

Importance of model

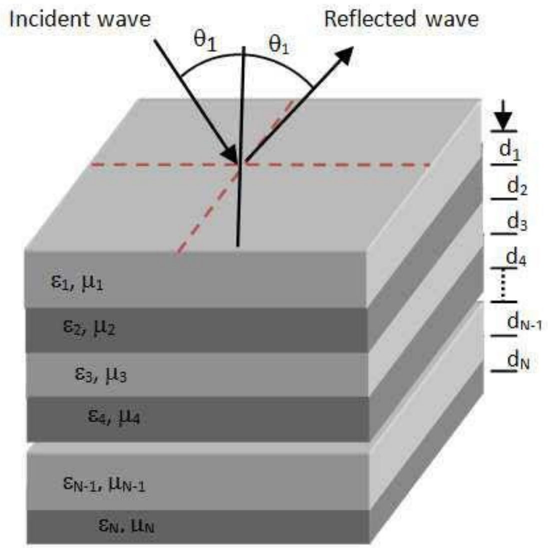

Model

- To construct the Fresnel equation, one needs the geometry of the sample. (thickness of each layer, and n, k values of each layer)
- Also, one assumes the homogeneity and flatness of the boundaries.
- In real samples, the inhomogeneity and roughness of the sample surfaces/boundaries leads to the failure of extracting n & k.
  ⇒ e.g. n,k values are different for different incidence angles
- One of the most used method for modeling the inhomogeneity & roughness is the effective medium approximation (EMA).

Experimentally measured: ψ & Δ

$$\rho \equiv \tan\psi \exp(i\Delta) \equiv \frac{r_p}{r_s} \equiv \left(\frac{E_{rp}}{E_{ip}}\right) \Big/ \left(\frac{E_{rs}}{E_{is}}\right)$$

$$\tan\psi = |r_p|/|r_s| \qquad \Delta = \delta_{rp} - \delta_{rs}$$

- To make the optical fitting more unique, the ψ & Δ are measured at several incidence angles (50°, 60°, 70°)
- Angles near the Brewster angle (~60°)⇒ to maximize the R_p and R_s difference
  $\theta_B(n) = \arctan(n)$; $\theta_B(1.3) \sim 52°$; $\theta_B(1.7) \sim 60°$; $\theta_B(2.0) \sim 63°$;

Fitting procedure

Goal: ***n*, *k* of film 2**

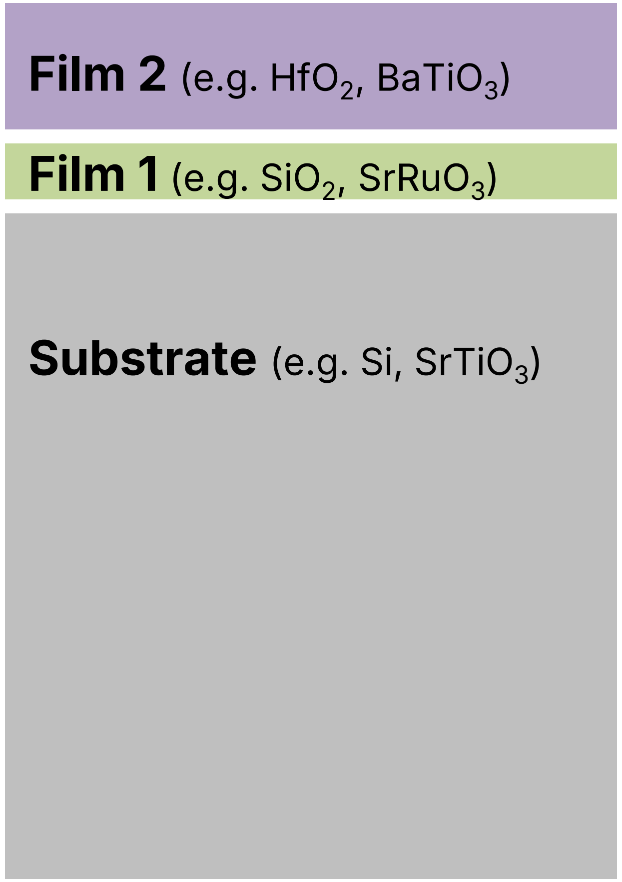

3) Measure Film 2 + Film 1 + substrate and calculate the optical constants of the film 2.

1) Obtain the optical constants of the substrate

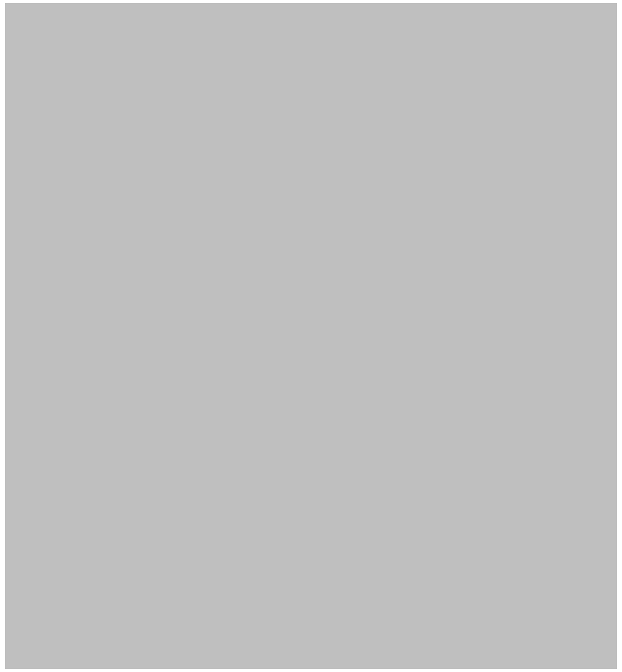

2) Measure Film 1 + substrate and calculate the optical constants of the film 1.

Angle dependence to check the ideality

- The optical constants are intrinsic physical properties and should not vary with incident angles.
- In the model, we always assume the homogeneous medium and atomically flat (<1 nm) surface.
- Real samples often fails to reach such high quality, leading to depolarization and geometric effects.
- To check if the sample qualities are acceptable for ellipsometry measurement, scan bulk material at various incident angles and check the *n*, *k* (or ϵ_1, ϵ_2) overlap.

- Inhomogeneity and surface roughness can be for some amount modelled with the effective medium approximation (EMA) theory.
  Material A: Our sample
  Material B: air

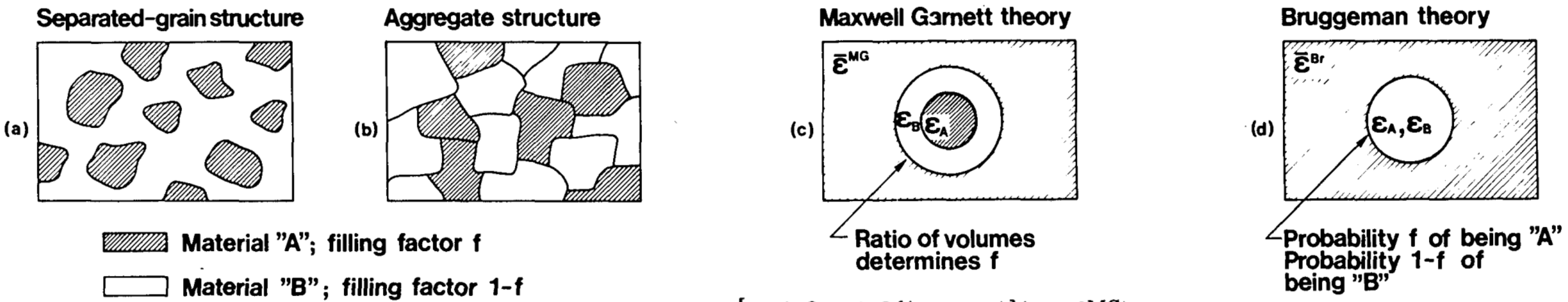

$$\bar{\varepsilon} = \varepsilon_B \frac{[\varepsilon_A + 2\varepsilon_B + 2f(\varepsilon_A - \varepsilon_B)](1 + \delta^{MG})}{[\varepsilon_A + 2\varepsilon_B - f(\varepsilon_A - \varepsilon_B)](1 - 2\delta^{MG})}$$

$$f\frac{\varepsilon_A - \bar{\varepsilon}}{\varepsilon_A + 2\bar{\varepsilon}} + (1-f)\frac{\varepsilon_B - \bar{\varepsilon}}{\varepsilon_B + 2\bar{\varepsilon}} + \delta^{Br}(\varepsilon_A, \varepsilon_B, \bar{\varepsilon}, f, b, \lambda) = 0$$

Niklasson *et al.*, Applied Optics **20**, 26 (1981)

Optical conductivity and electronic band

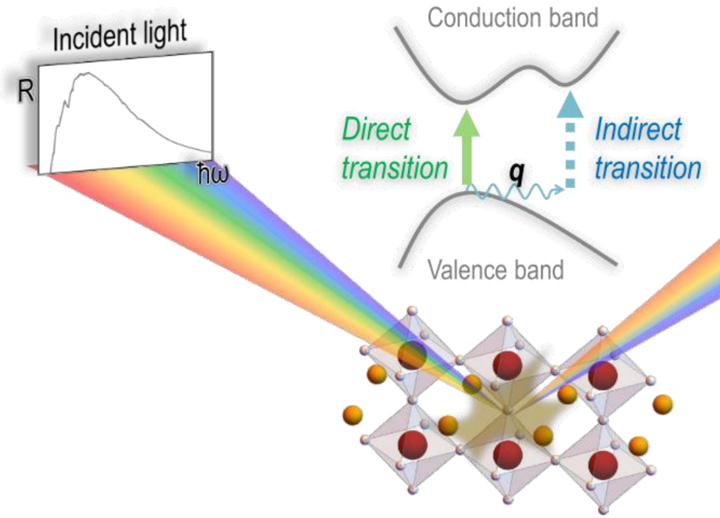

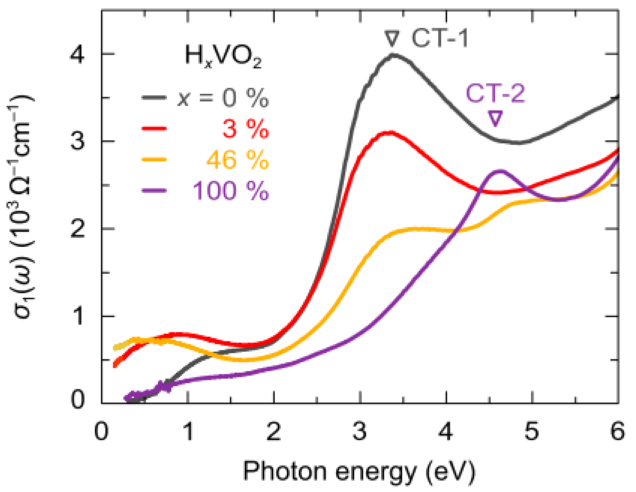

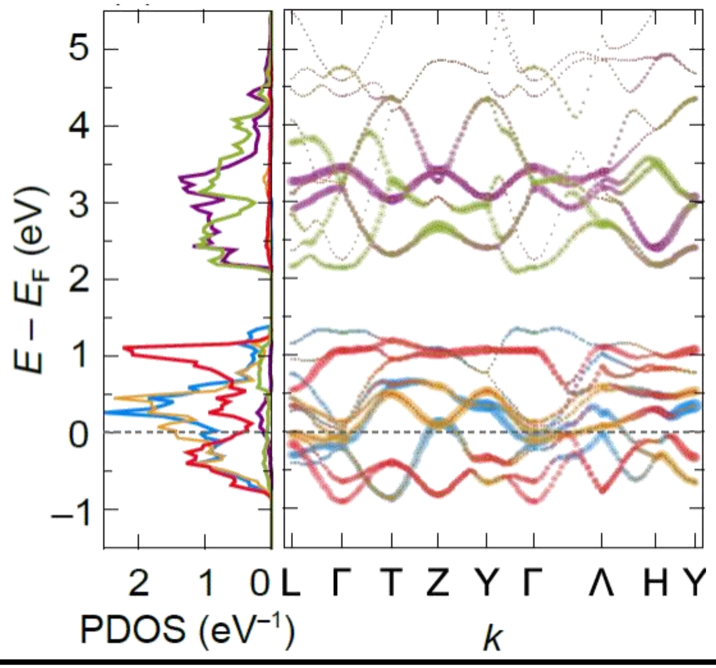

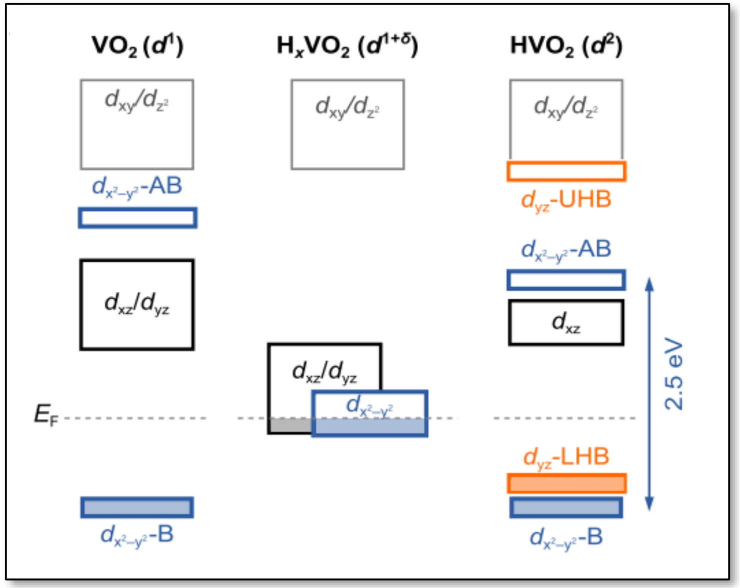

Interband optical transition

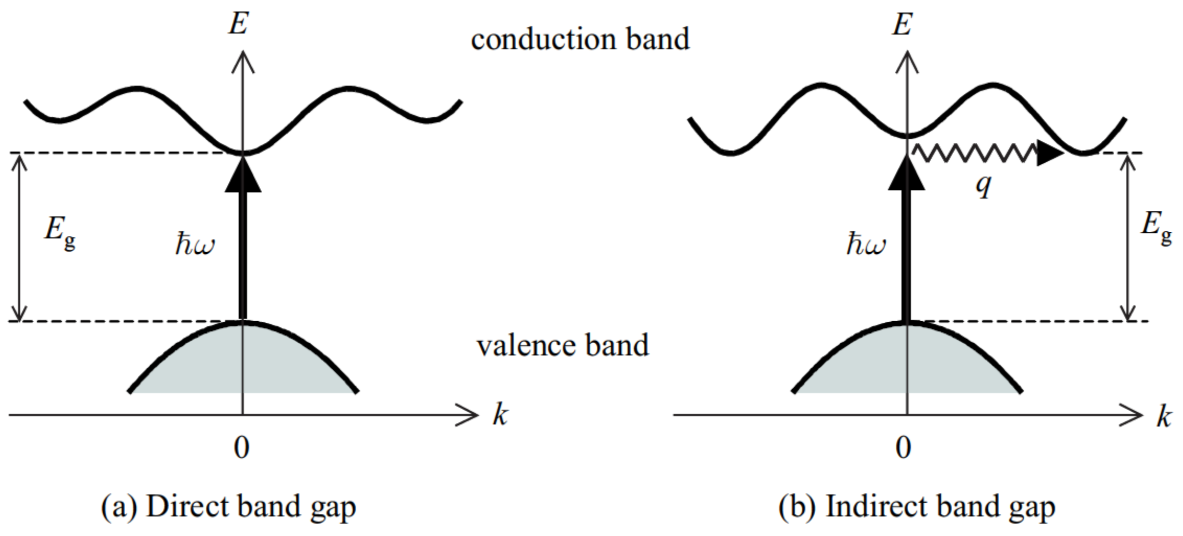

Fermi's Golden Rule

$$W_{\mathrm{i}\to\mathrm{f}} = \frac{2\pi}{\hbar}|M|^2 g(\hbar\omega)$$

$g(\hbar\omega)$ is the joint density of state, which accounts for the number of occupied–unoccupied electronic state pairs separated by a given photon energy.

Matrix element

$$M = \langle \mathrm{f}|H'|\mathrm{i}\rangle = \int \psi_\mathrm{f}^*(\boldsymbol{r})\, H'(\boldsymbol{r})\, \psi_\mathrm{i}(\boldsymbol{r})\, \mathrm{d}^3\boldsymbol{r}$$

$$H' = -\boldsymbol{p}_\mathrm{e}\cdot\boldsymbol{\mathcal{E}}_{\mathrm{photon}}$$

p_e is the electric dipole

Tauc plot

- Direct band gap edge

$$\alpha(\hbar\omega) \propto (\hbar\omega - E_\mathrm{g})^{1/2}$$

- Indirect band gap edge

$$\alpha^{\mathrm{indirect}}(\hbar\omega) \propto (\hbar\omega - E_\mathrm{g} \mp \hbar\Omega)^2$$

Interband optical transition

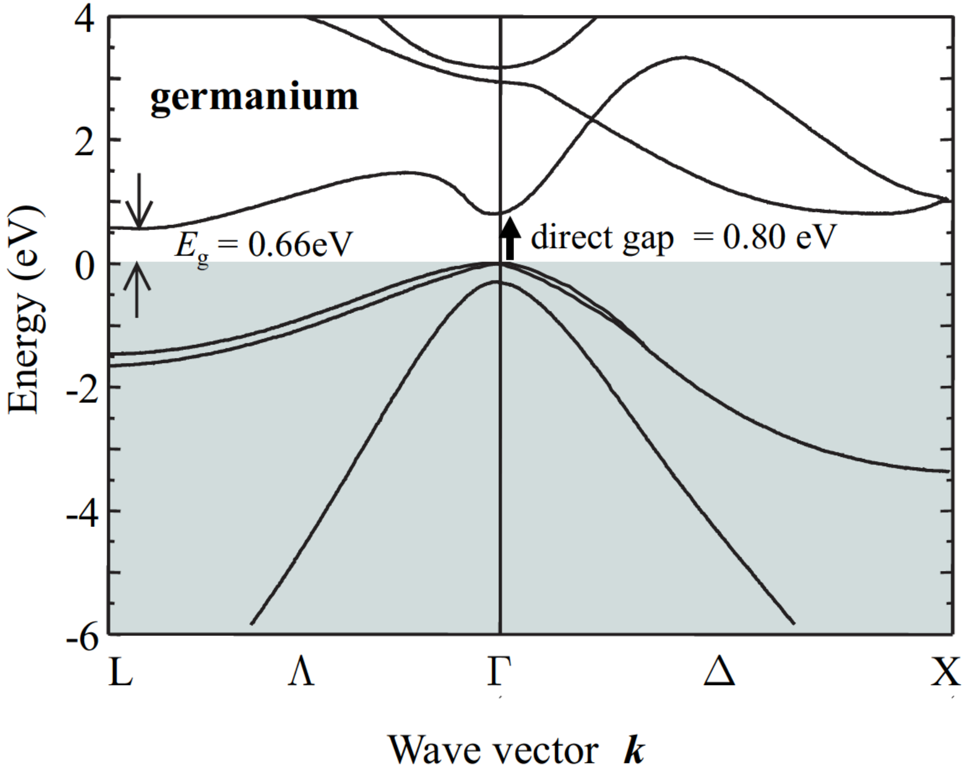

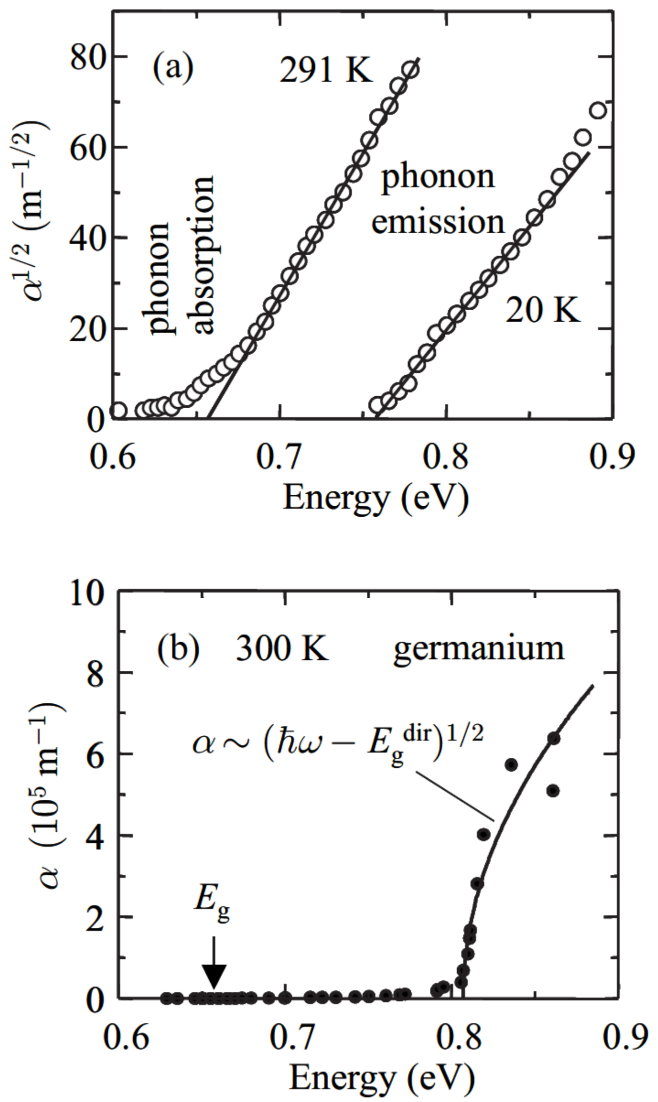

Note. the single band picture

- The band gap edge and the types of the band gap can be obtained.

Optical responses from topological materials

Phys. Status Solidi B **258**, 2000027 (2021)

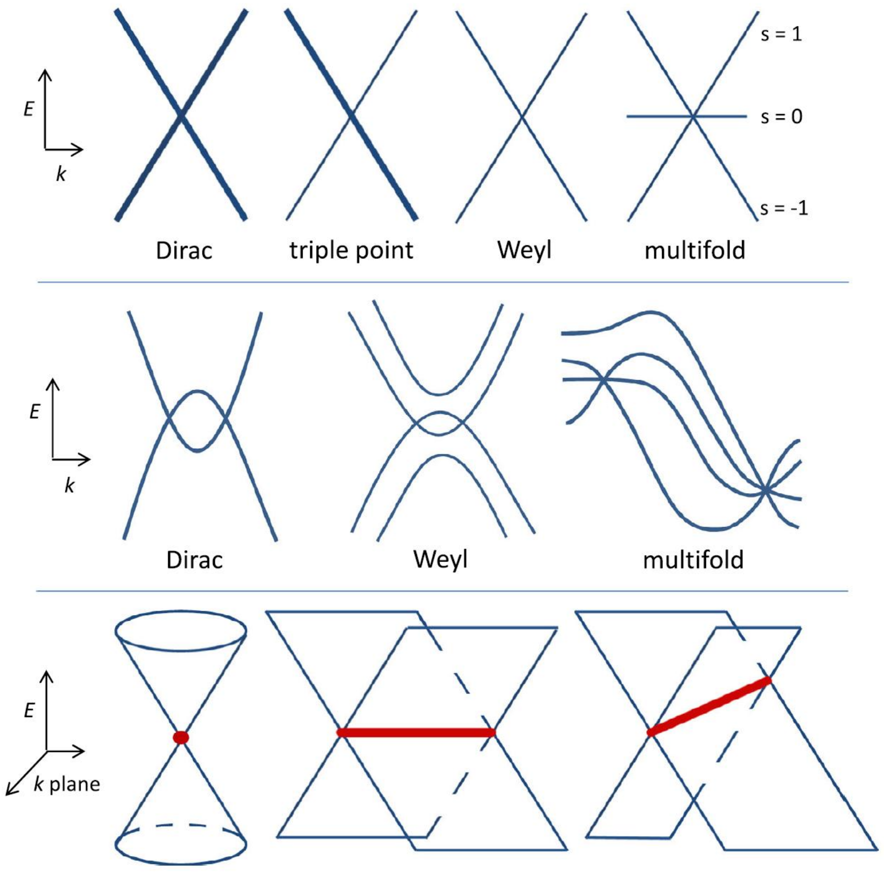

Kubo-Greenwood formula

D: JDOS

$$\sigma_1(\omega) = \frac{\pi e^2}{m^2 \omega} |\mathbf{p}_{s's}(\omega)|^2 D_{s's}(\hbar\omega)$$

p: momentum operator

$$\sigma_1^{\mathrm{IB}}(\omega) \propto \omega^{(d-2)/z}$$

d: dimension
z=1 for 3D Dirac and Weyl

$$\sigma_1^{\mathrm{IB}}(\omega) = \frac{e^2 N_{\mathrm{W}}}{12h} \frac{\omega}{v_{\mathrm{F}}}$$

N_W: # of Weyl nodes

$$= \frac{e^2 N_{\mathrm{W}}}{12h} \frac{\omega}{v_{\mathrm{F}}} \theta\{\hbar\omega - 2\mu\}$$

Optical responses from topological materials

LETTERS

nature physics

Dirac charge dynamics in graphene by infrared spectroscopy

Z. Q. LI[1]*, E. A. HENRIKSEN[2], Z. JIANG[2,3], Z. HAO[4], M. C. MARTIN[4], P. KIM[2], H. L. STORMER[2,5,6] AND D. N. BASOV[1]

$$\sigma_1^{\mathrm{IB}}(\omega) \propto \omega^{(d-2)/z}$$

Graphene
2D Dirac
(d = 2, z =1)

Universal 2D conductivity

$$\sigma_1(\omega,\, V_{\mathrm{CN}}) = \pi e^2/2h$$

Note. Pauli blocking below the E_F

Graphene device (Voltage control) + FTIR

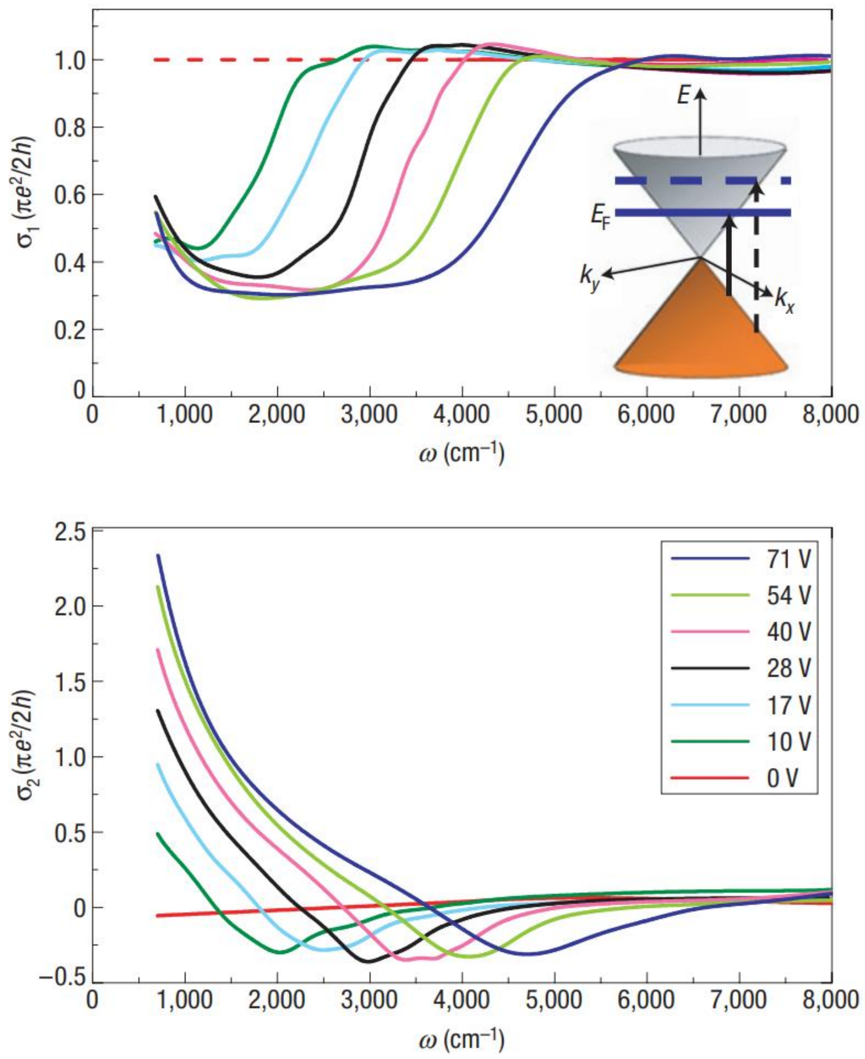

Optical responses from topological materials

Model calculation
PRB **93**, 085442 (2016).

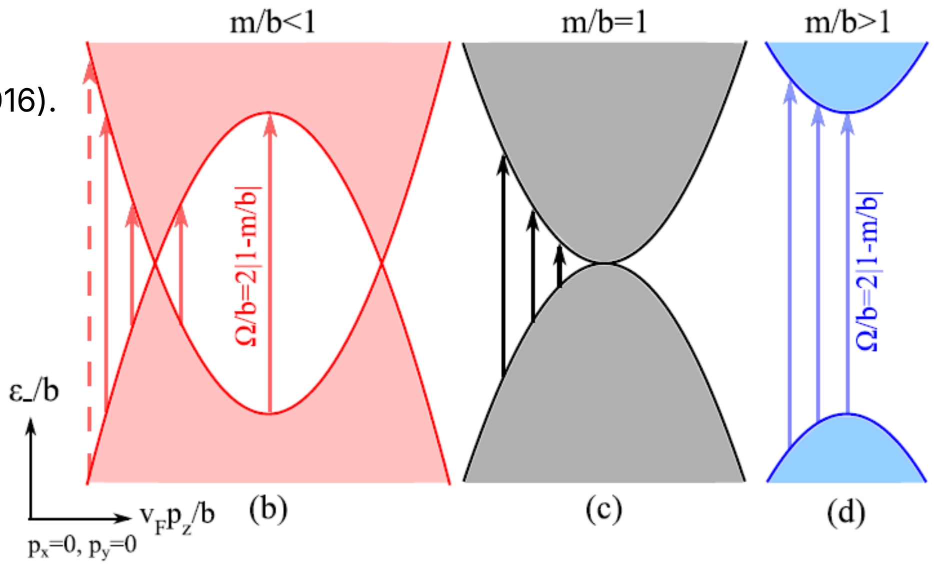

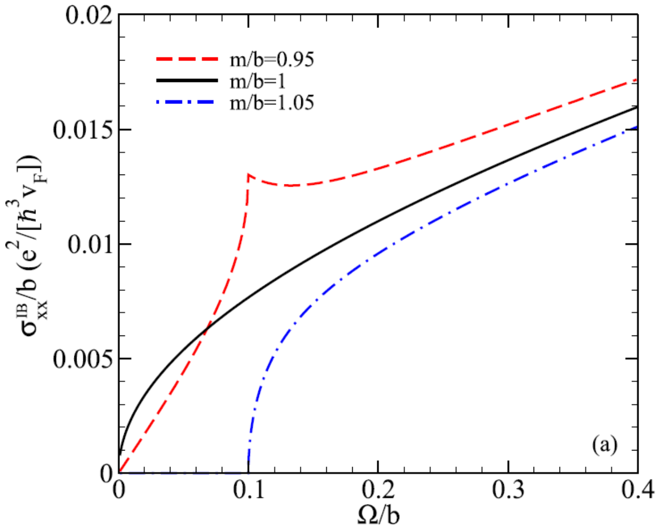

Linear conductivity

TaAs (3D Weyl)
PRB 93, 121110(R) (2016).

$$\sigma_1^{\text{IB}}(\omega) \propto \omega^{(d-2)/z}$$

(d = 3, z =1) $\Rightarrow$ $\sigma \propto \omega$

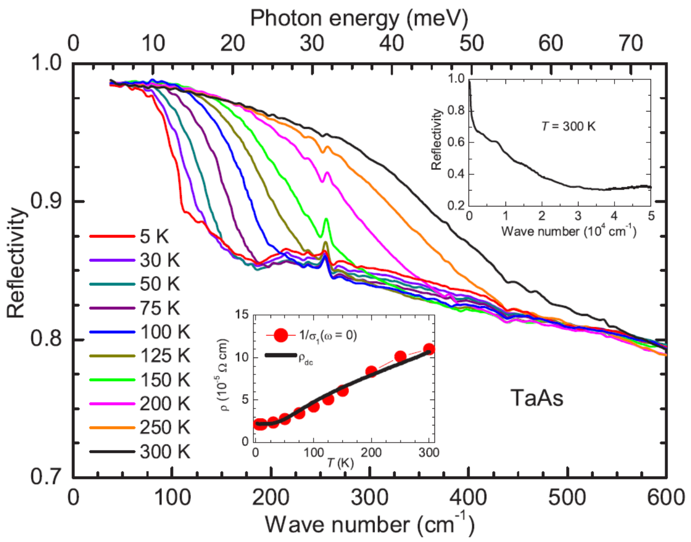

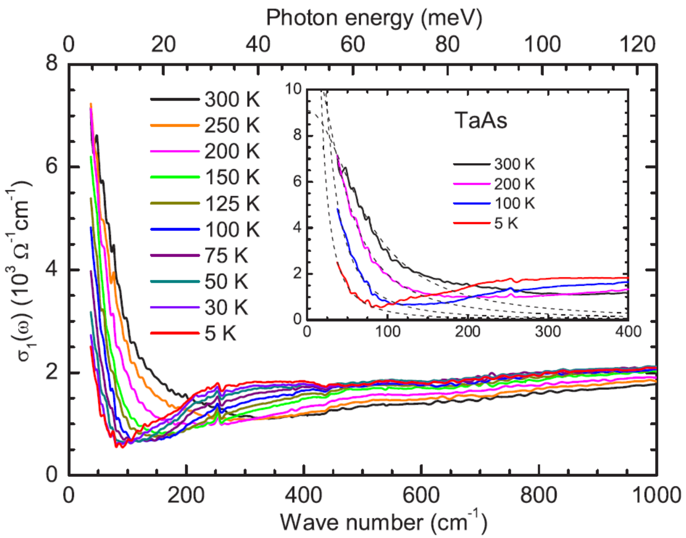

Optical responses from topological materials

Cd_3As_2(3D Dirac), PRB 93, 121202 (2016).

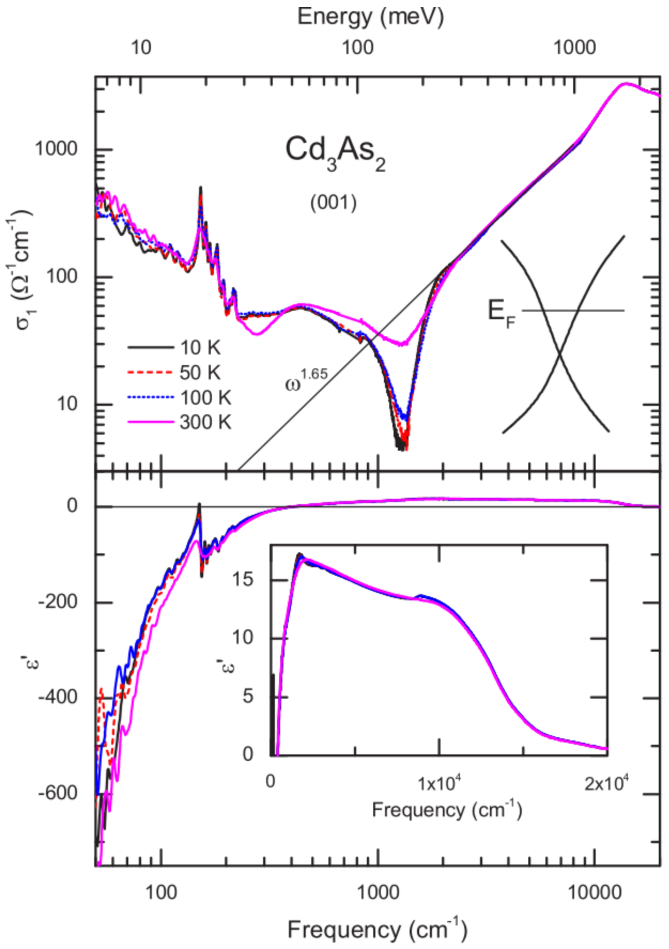

NbP (Type-I Weyl, 3D), PRB 98, 195203 (2018).

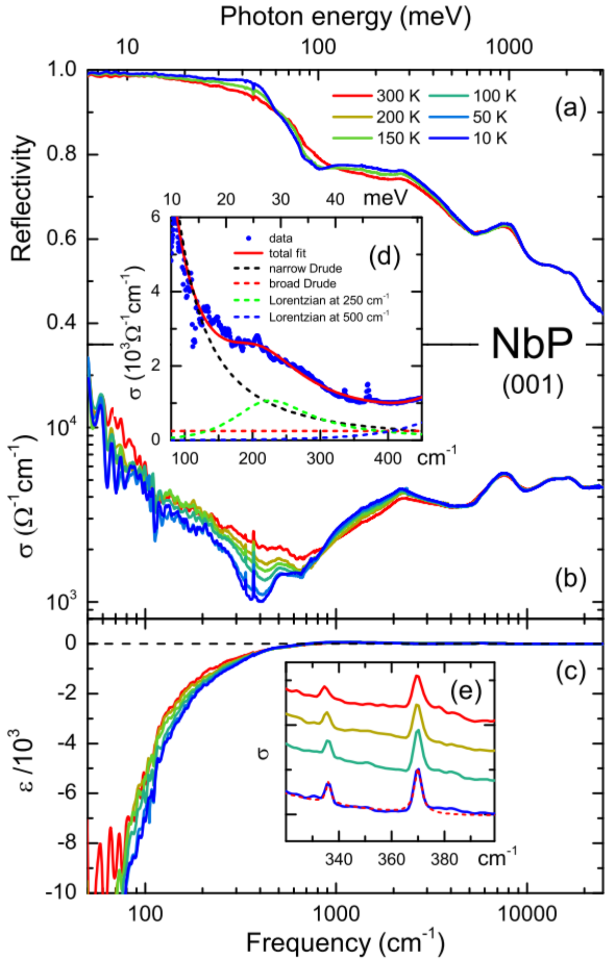

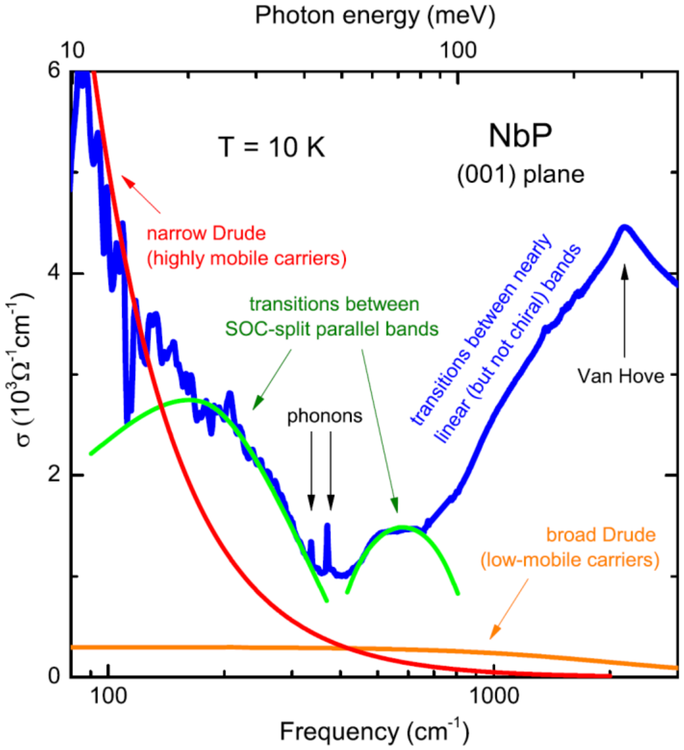

Optical responses from strongly correlated band

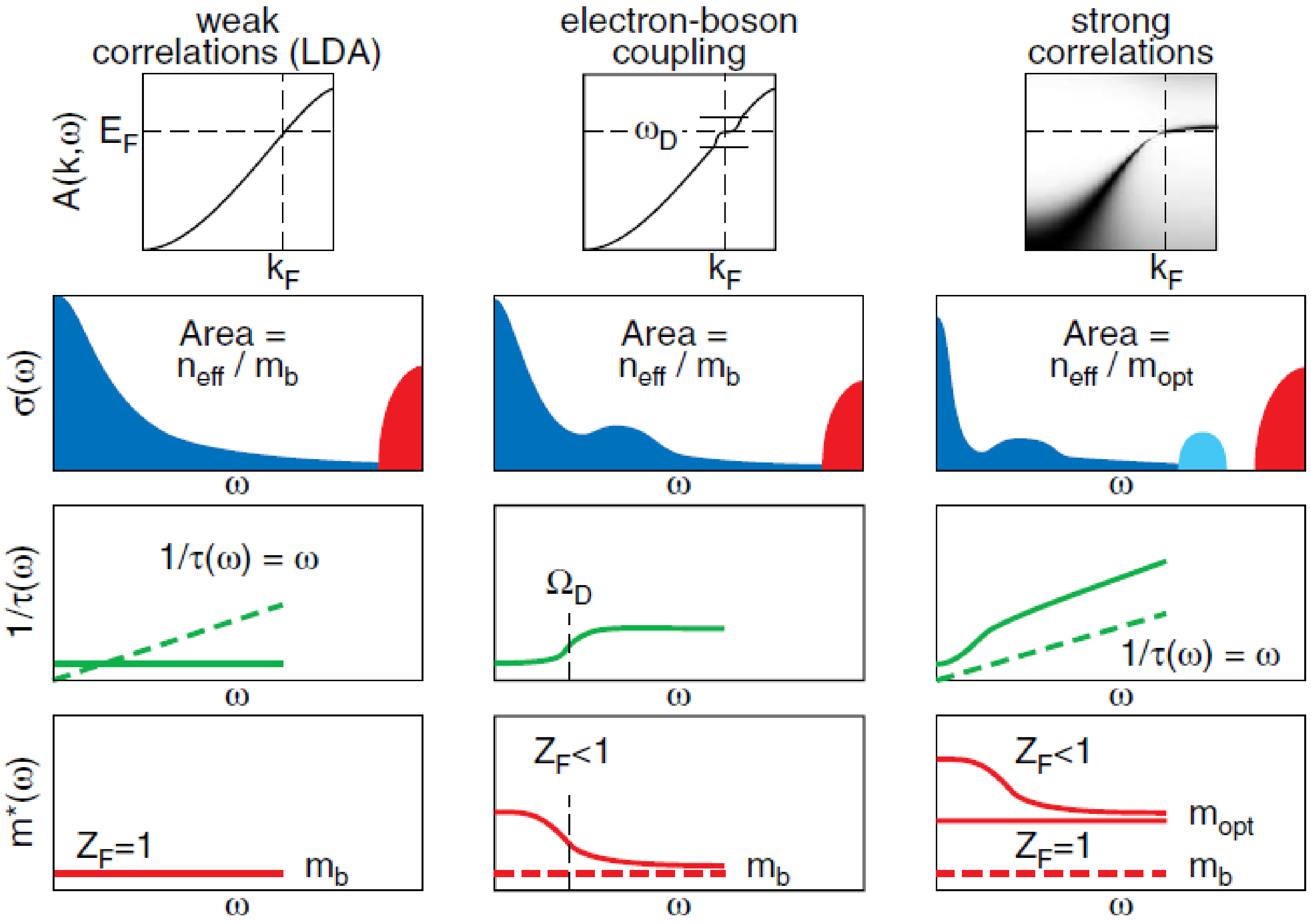

$m_{eff}/m_b \sim 2$

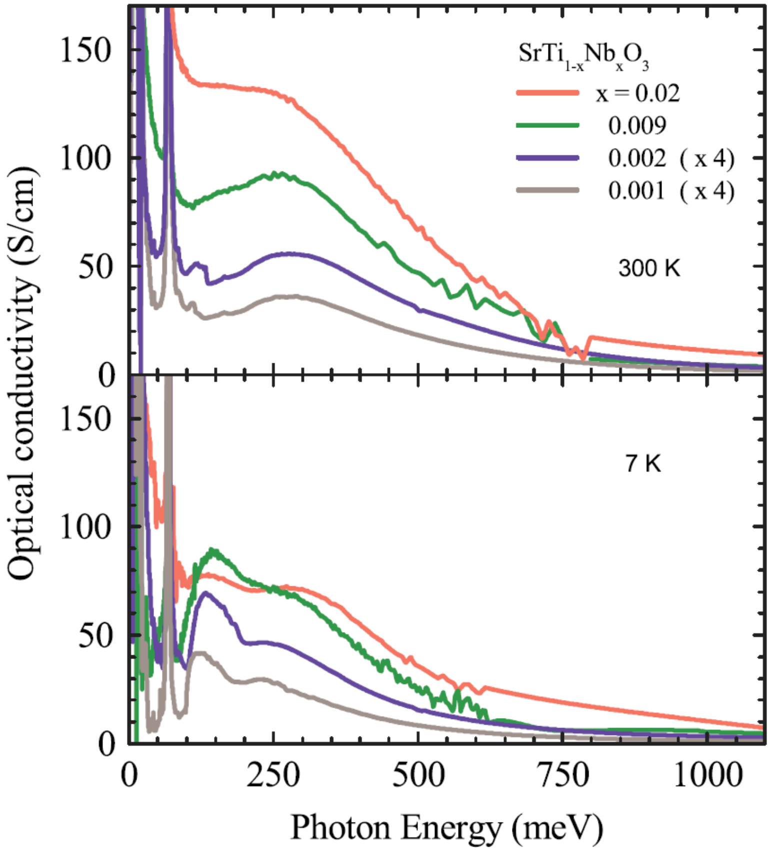

Basov *et al.*, Electrodynamics of correlated electron materials, Rev. Mod. Phys. **83**, 471 (2011)

Mott transition

Hubbard model

$$H = -\sum_{<i,j>\sigma} t_{ij} c_{i\sigma}^{\dagger} + U \sum_{i} n_{i\uparrow} n_{i\downarrow}$$

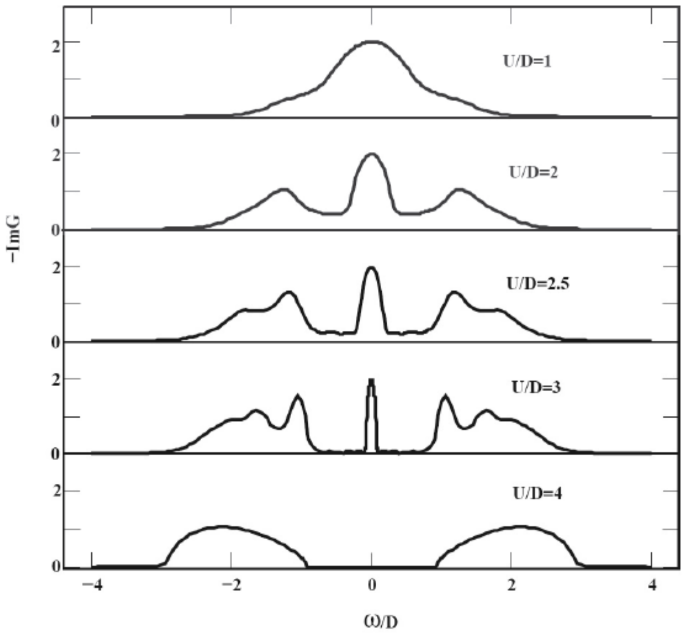

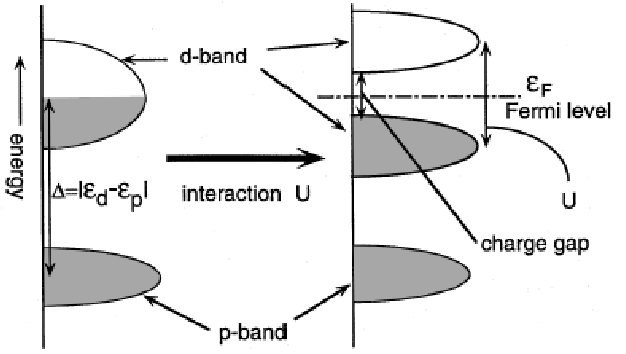

(a) Mott-Hubbard Insulator

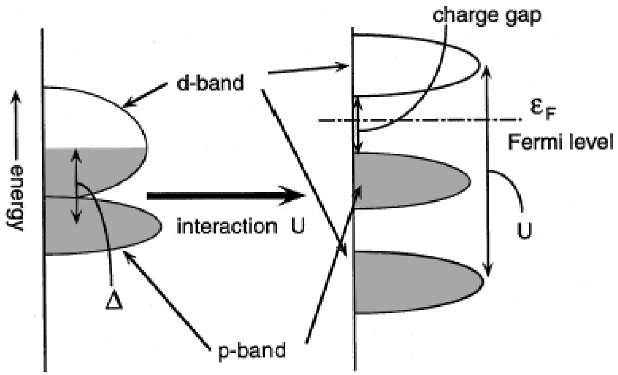

(b) Charge Transfer Insulator

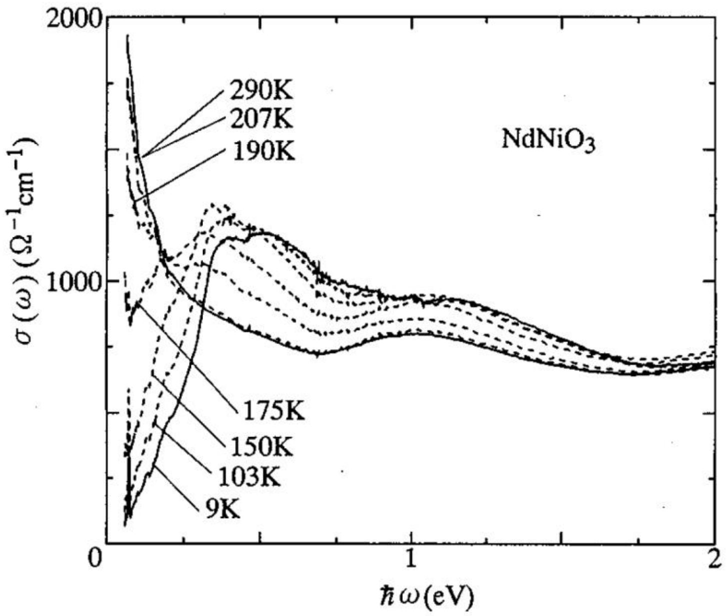

FIG. 86. Temperature dependence of optical conductivity spectra of $NdNiO_3$. From Katsufuji *et al.*, 1995.

Spectral weight transfer

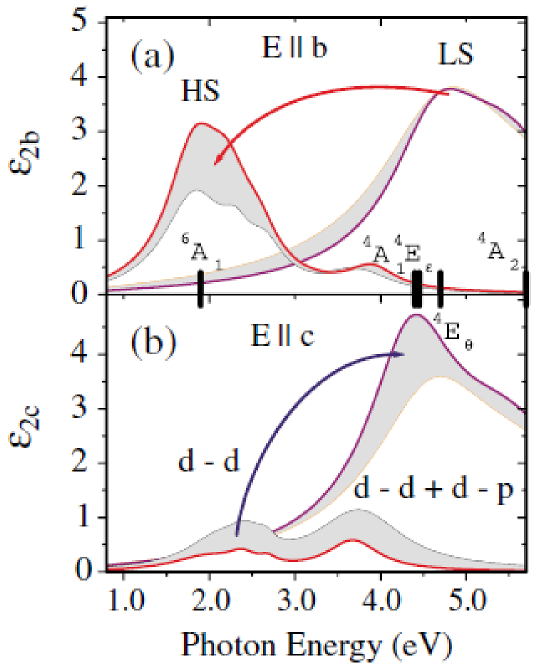

FIG. 31 (color online). Summary of the optical response of $LaMnO_3$ upon crossing from the orbitally ordered state to the antiferromagnetic state. (a) The imaginary part of the dielectric function ϵ_{2b} along the *b* axis. As the temperature decreases below T_N, there is a transfer of spectral weight from the low-spin (LS) to high-spin (HS) configuration which is consistent with what is expected for *d*-*d* intersite transition. (b) The imaginary part of the dielectric function ϵ_{2c} along the *c* axis. From Kovaleva *et al.*, 2004.

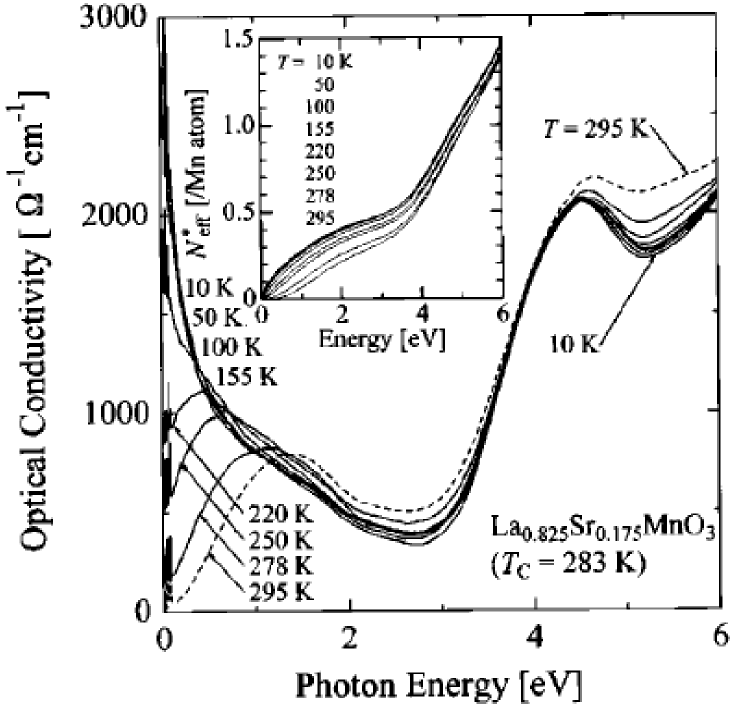

FIG. 32. σ_1 as a function of photon energy for various temperatures measured on a cleaved single crystal of $La_{0.825}Sr_{0.175}MnO_3$. The polaron peak at ~1 eV gradually redshifts with decreasing temperature to a Drude peak. The inset shows the integrated spectral weight as a function of energy for various temperatures. From Takenaka *et al.*, 1999.

Revealing electronic band structure

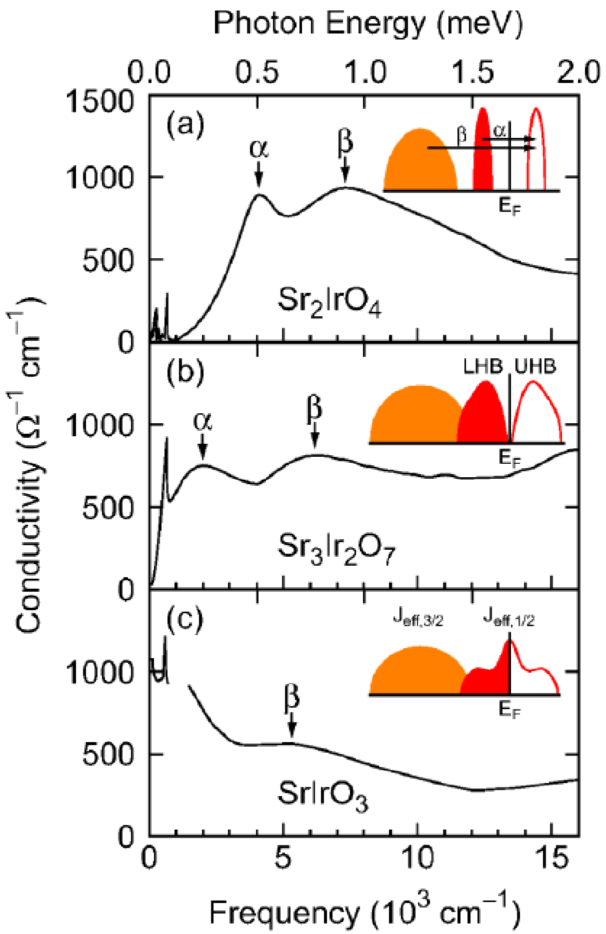

FIG. 38 (color online). Optical conductivity of the Ruddlesden-Popper series $Sr_{n+1}Ir_nO_{3n+1}$, where $n = 1$, 2, and ∞. The insets sketch the $t2g$ density of states in the three materials. From Moon *et al.*, 2008.

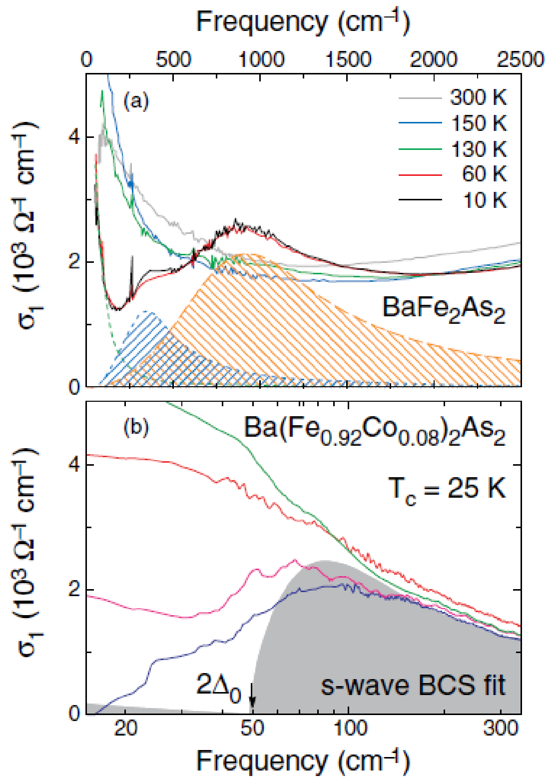

FIG. 47 (color online). (a) Optical conductivity of $BaFe_2As_2$ from room temperature, and across the antiferromagnetic transition around 140 K, down to 10 K. The partial gap due to SDW is clearly visible. Hu *et al.* (2008, 2009) associated the two peaks depicted with the excitations across the SDW gap. (b) Low-frequency conductivity of $Ba(Fe_{0.92}Co_{0.08})_2As_2$ above and below the superconducting transition $T_c = 25$ K. The curve given by the shaded area is calculated using the theory of Mattis and Bardeen (1958) for the lowest temperature with a gap of $2\Delta_0^{(1)} = 50$ cm^{-1}. From Wu *et al.*, 2010b.

Contents

IR, Raman and PL

	IR	Raman	PL (Photoluminescence)
Principle	Light **absorption** Vibrational excitation	Light **inelastic scattering** (Stokes / anti-Stokes)	Light absorption → electronic excitation → **re-emission**
Selection rule	$\partial\mu/\partial Q \neq 0$ Change in dipole moment during vibration required	$\partial\alpha/\partial Q \neq 0$ Change in polarizability during vibration required	Allowed electronic transition (parity & spin selection rules) $\Delta E = h\nu$
Mutual exclusion	**Rule of Mutual Exclusion** In centrosymmetric molecules, IR active and Raman active modes are mutually exclusive		Not applicable
Light source	Infrared light (far-IR, mid-IR, near-IR)	Visible / NIR laser	UV / visible laser
Detected signal	Transmission / reflection spectrum	Scattering spectrum	Emission spectrum

Review: Electric dipole and polarizability

<u>Dipole moment</u>

permanent dipole

$$\mathbf{p}_{\text{dipole}} = q\,\mathbf{d}$$

$$\langle \Psi_f \mid e\mathbf{r} \mid \Psi_i \rangle \neq 0$$

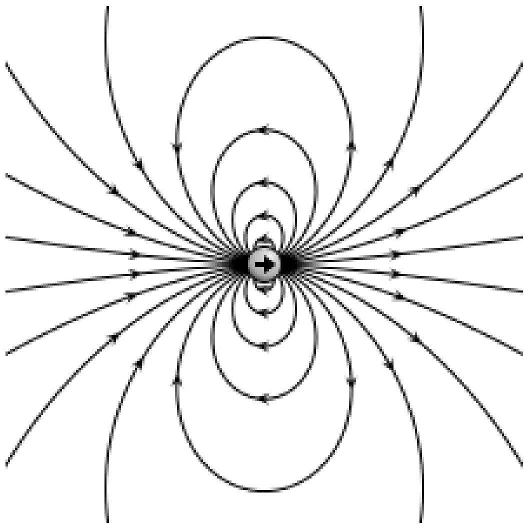

- Intrinsic/permanent separation of charge
- Present in the absence of an **E**-field
- Probe: Infrared spectroscopy (absorption/reflection)
  Photoluminescence (emission)

<u>Polarizability</u>

induced dipole

$$\mathbf{p}_{\text{induced}} = \overleftrightarrow{\alpha}\,\mathbf{E}$$

Note. E_x can induce P_y and etc. $\Longrightarrow$ tensor

$$\left\langle \Psi_f \left| \frac{\partial \alpha_{ij}}{\partial Q} \right| \Psi_i \right\rangle \neq 0$$

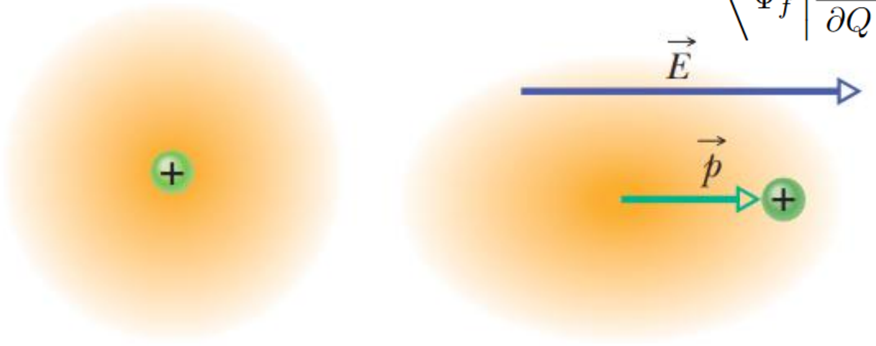

- Tendency of a charge to distort under external **E**-field.
- Disappears in the absence of an **E**-field
- Probe: Raman scattering
  (re-emission from induced dipole)

Phonon dispersion of a diatomic chain

$$\omega_{\pm}^2 = K\left(\frac{1}{m_1}+\frac{1}{m_2}\right) \pm K\sqrt{\left(\frac{1}{m_1}+\frac{1}{m_2}\right)^2 - \frac{4\sin^2\frac{ka}{2}}{m_1 m_2}},$$

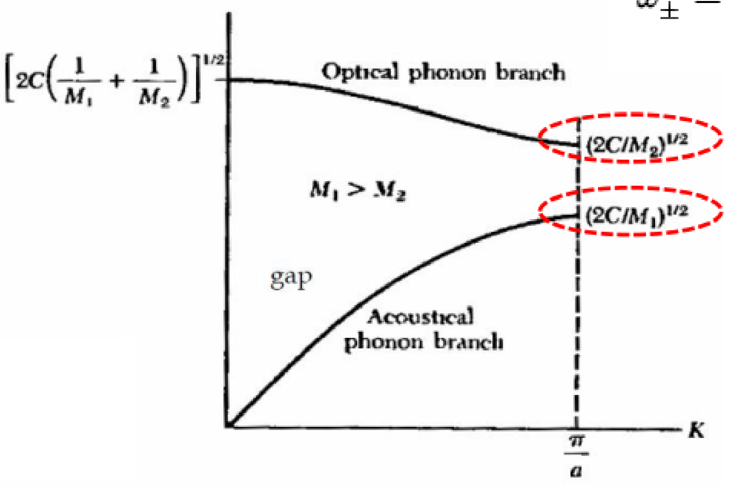

»For the shortest waves in acoustic branch the lighter atoms are still and mo
atoms oscillate; in the optical branch the situation is inverse.

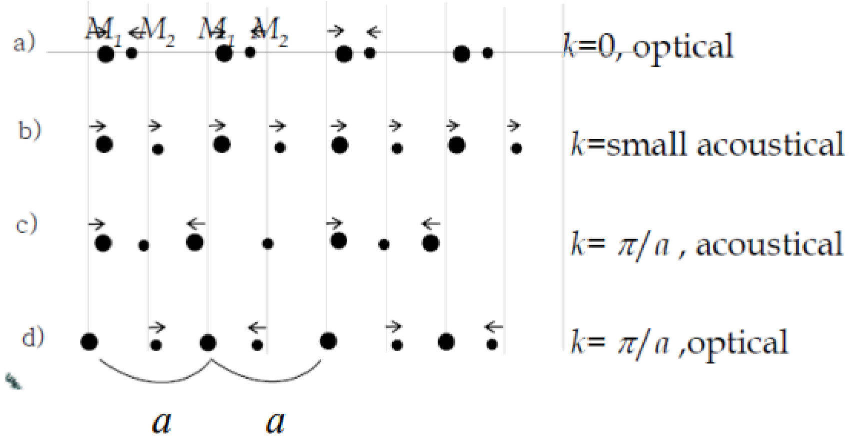

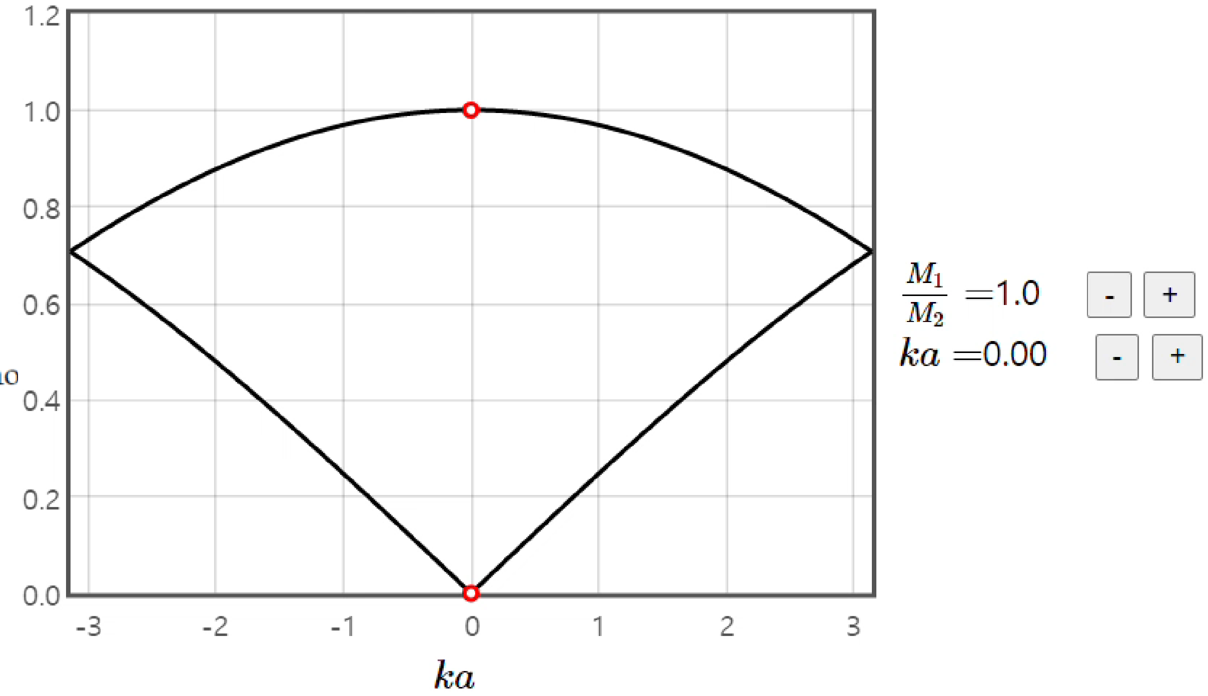

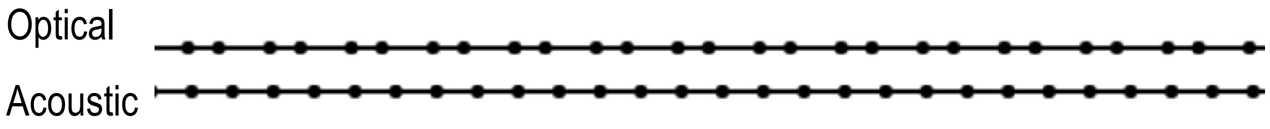

Raman- and IR-activity of phonon

Phonon dispersion
- inelastic neutron scattering
- x-ray scattering

Optical mode

- **IR-active**
  - Reflection/absorption
- **Raman-active**
  - Raman scattering
  - pump-probe ΔR

Acoustic mode
- Brillouin scattering

Silent mode
- higher-order Raman scattering

Q: Normal coordinate
(quantifies the displacement of all atoms in a given vib. Normal mode)
Q = 0: equilibrium
Q = ±Q: two opposite extremes of the motion

μ: dipole moment
α: polarizability

Linear Triatomic Molecule

	ν_1 in-phase stretch	ν_3 out-of-phase stretch	ν_2 bending
Mode of vibration	$-Q$ $Q=0$ $+Q$	$-Q$ $Q=0$ $+Q$	$-Q$ $Q=0$ $+Q$
Dipole moment			
Variation of dipole moment with normal coordinate (schematic)	$\partial\mu/\partial Q = 0$	$\partial\mu/\partial Q \neq 0$	$\partial\mu/\partial Q \neq 0$
Infrared activity	No	Yes	Yes
Polarizability ellipsoid			
Variation of polarizability with normal coordinate (schematic)	$\partial\alpha/\partial Q \neq 0$	$\partial\alpha/\partial Q = 0$	$\partial\alpha/\partial Q = 0$
Raman activity	Yes	No	No

Raman spectroscopy

General properties

- Measures light inelastically scattered off materials ⇛ very weak in intensity
- Inelastic due to loss/gain to molecular and lattice vibrations
- Exhibits as a sideband from incident laser wavelength (visible/NIR used)
- Coexists with photoluminescence (PL) signal of which the intensity is 10^6–10^8 stronger.

Classical understanding of Raman scattering

① The laser's electric field induces an oscillating dipole in the molecule ⟹ $\mu = \alpha E$

② The polarizability is modulated by the molecular vibration at ω_{vib} ($\alpha_1 \propto \partial\alpha/\partial Q$) ⟹ $\alpha = \alpha_0 + \alpha_1\cos(\omega_{vib}t)$

③ The incident laser field oscillates at ω_{Laser} ⟹ $E = E_0\cos(\omega_L t)$

④ $\mu = \alpha E$ mixes the two frequencies ⟹ multiplying the modulated α by the oscillating E gives: $\cos(\omega_{vib}t)\cdot\cos(\omega_{Laser}t)$ term

⑤ Using trig identity, one gets three components in the scattered light:
ω_{Laser} : Rayleigh (elastic scattering, no energy exchange)
$\omega_{Laser} - \omega_{vib}$: Stokes (light gives one vibrational quantum to the molecule)
$\omega_{Laser} + \omega_{vib}$: Anti-Stokes (light takes energy from an already-vibrating molecule)

⑥ If $\alpha_1 = 0$ ($\partial\alpha/\partial Q = 0$), the sidebands vanish ⟹ Determines the Raman activity selection rule

Scattering spectrum

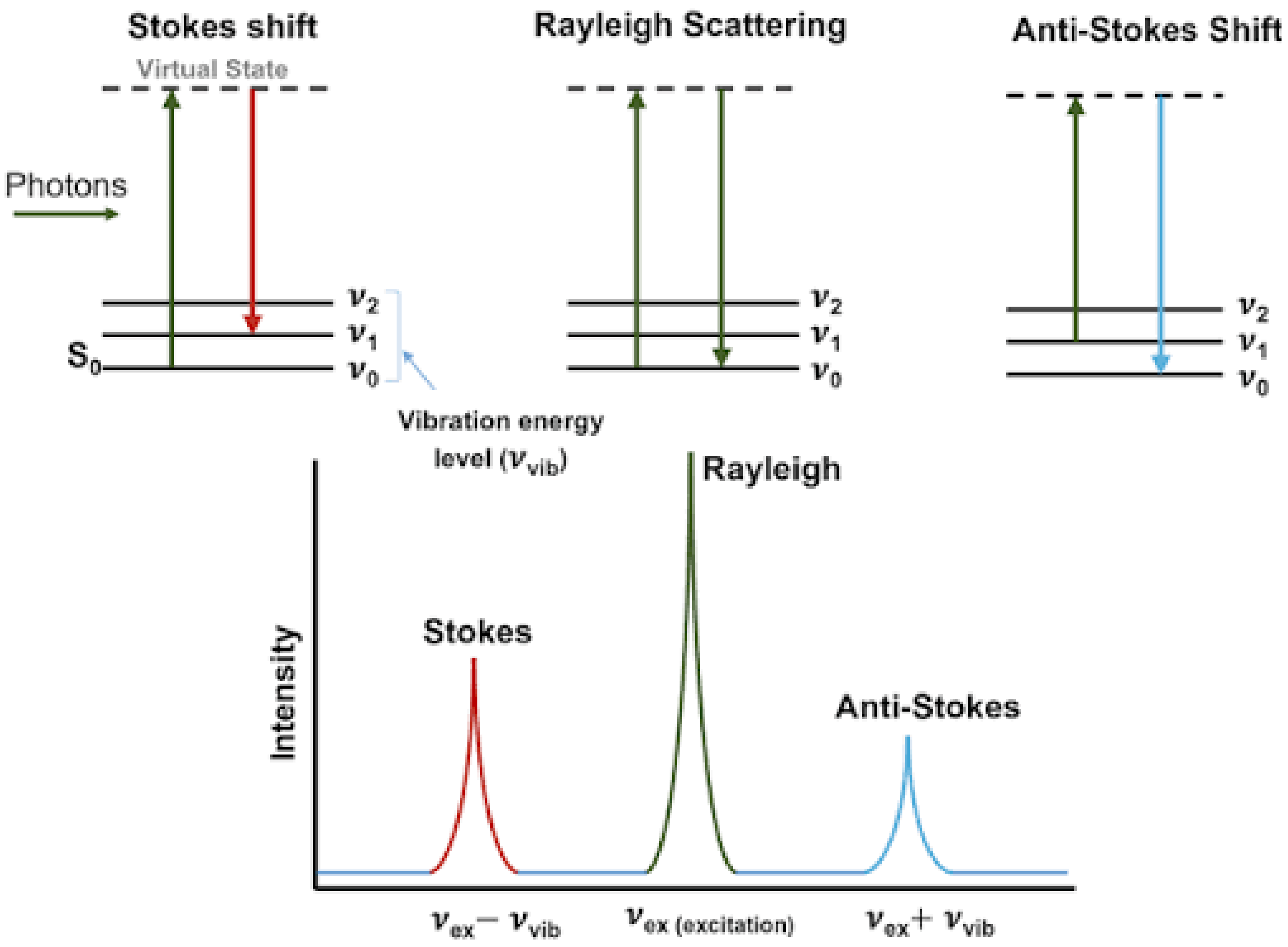

Fig. from Sci. Rep. **10**, 11692 (2020)

Quantum mechanical mechanism of Raman scattering

① Two-photon scattering process via a short-lived virtual state*, and immediately re-emits a photon while landing in a final vibrational state *Superposition of all real eigenstate E_n (scaled by KHD term)

② Energy conservation
$\hbar\omega_{\mathrm{scattered}} = \hbar\omega_{\mathrm{Laser}} - (E_{\mathrm{f}} - E_{\mathrm{i}})$

③ $\psi_{\mathrm{i}} = \psi_{\mathrm{f}}$ Rayleigh (elastic)
$v \rightarrow v+1$ Stokes (gains one vibrational quantum $\hbar\omega_{vib}$)
$v+1 \rightarrow v$ Anti-Stokes (loses a quantum $\hbar\omega_{vib}$)

④ Scattering amplitude proportional to:
(Fermi Golden rule in 2nd order perturbation, or KHD Kramers-Heisenberg-Dirac term)

$$\left\langle \Psi_f \left| \frac{\partial \alpha_{ij}}{\partial Q} \right| \Psi_i \right\rangle \neq 0$$

⟹ Consistent with classical selection rule $\partial\alpha/\partial Q \neq 0$

⑤ Resonance Raman
Strong intensity at $\hbar\omega_{\mathrm{Laser}}$ ~ (one of the) E_n
⟹ change the laser source

⑥ Non-contact temperature measurement using Boltzmann distribution
Stokes: initial state (v_0) in the ground state (many!)
Anti-stokes: in the excited state (a few) ⟹ the occupation number increases at higher temperature
$N(v_1)/N(v_0) = \exp(\hbar\omega_{\mathrm{vib}}/k_{\mathrm{B}}T)$

Phonons measured using FTIR

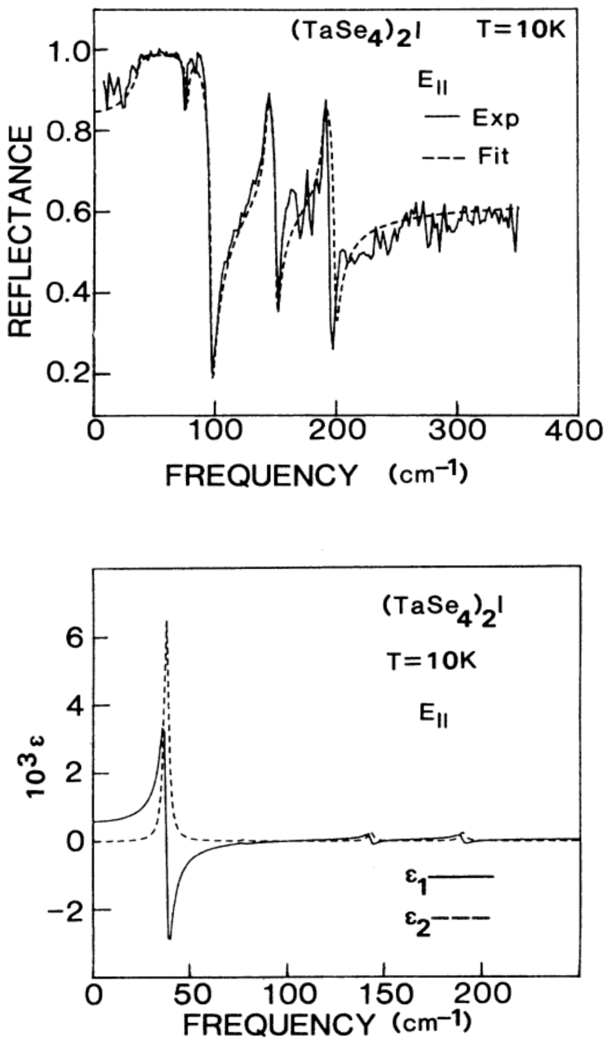

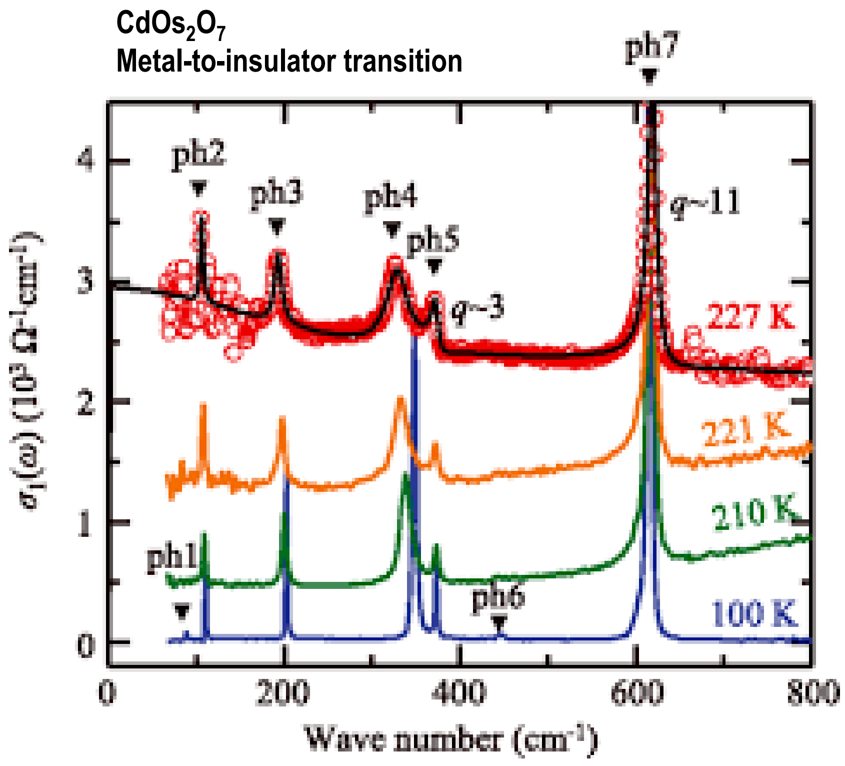

PRL **118**, 117201 (2017).

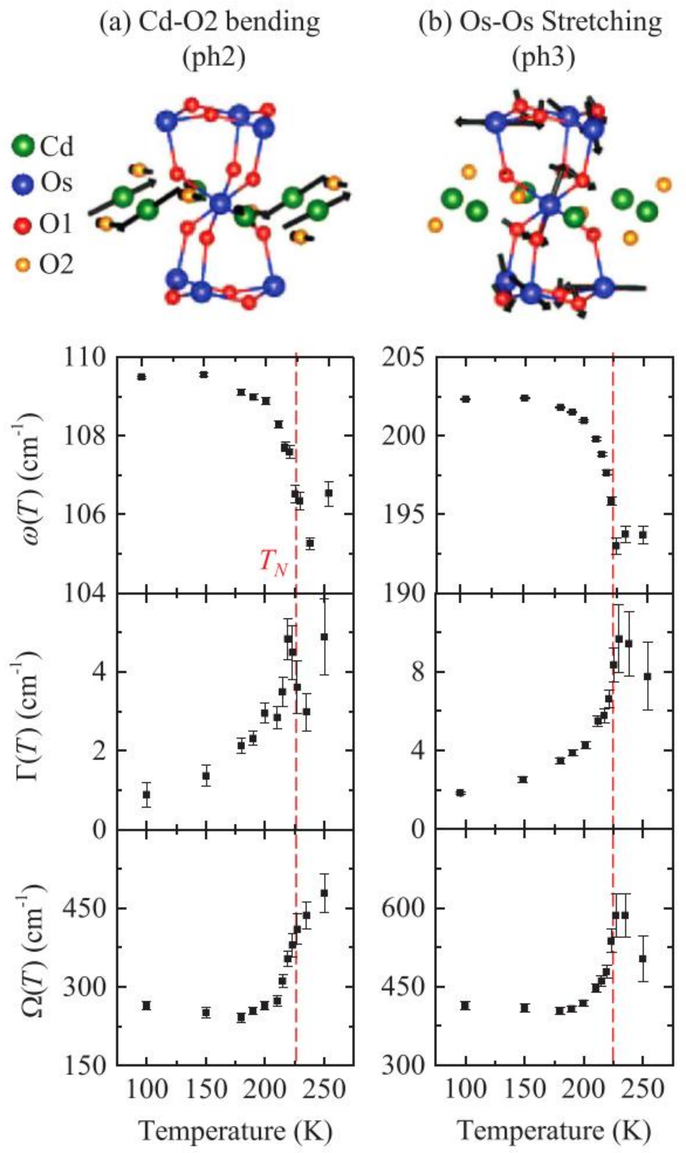

Phonons measured using FTIR

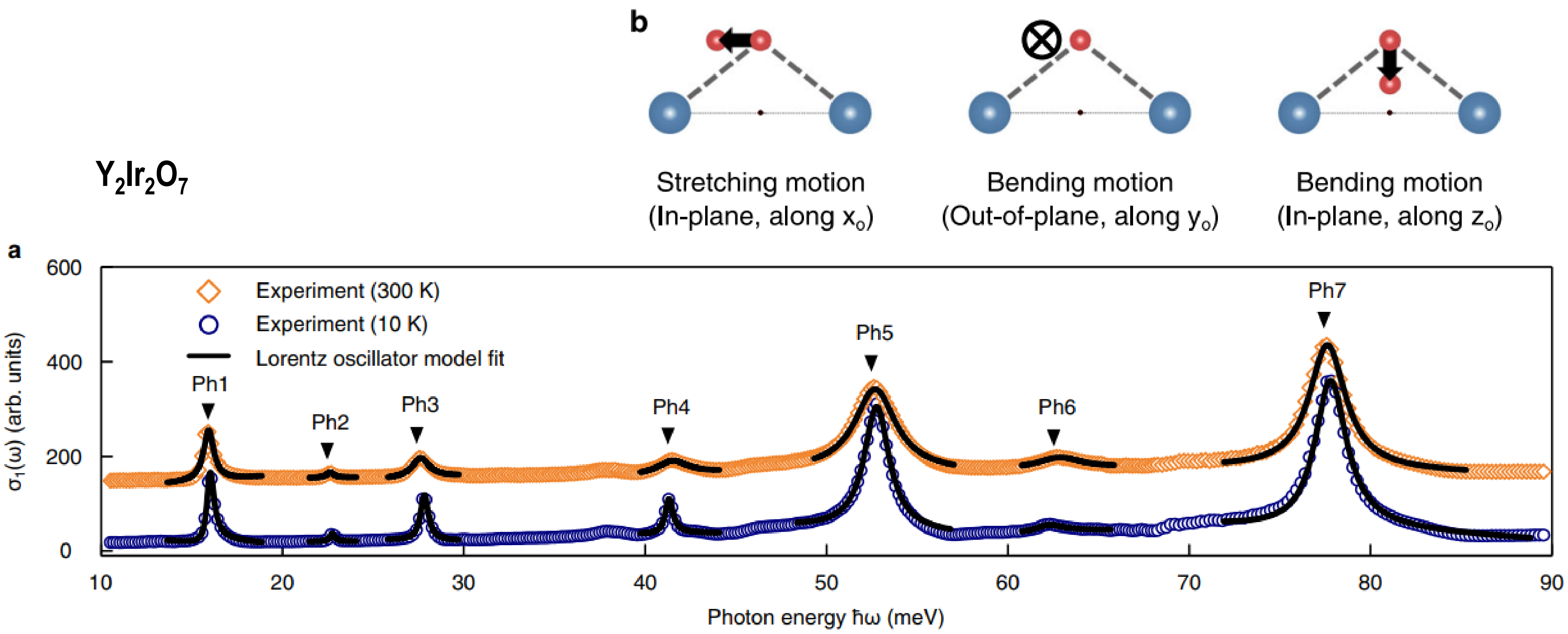

J. Son *et al.*, npj Quantum Materials **4**, 17 (2019).

Phonons measured using Raman

MoS_2

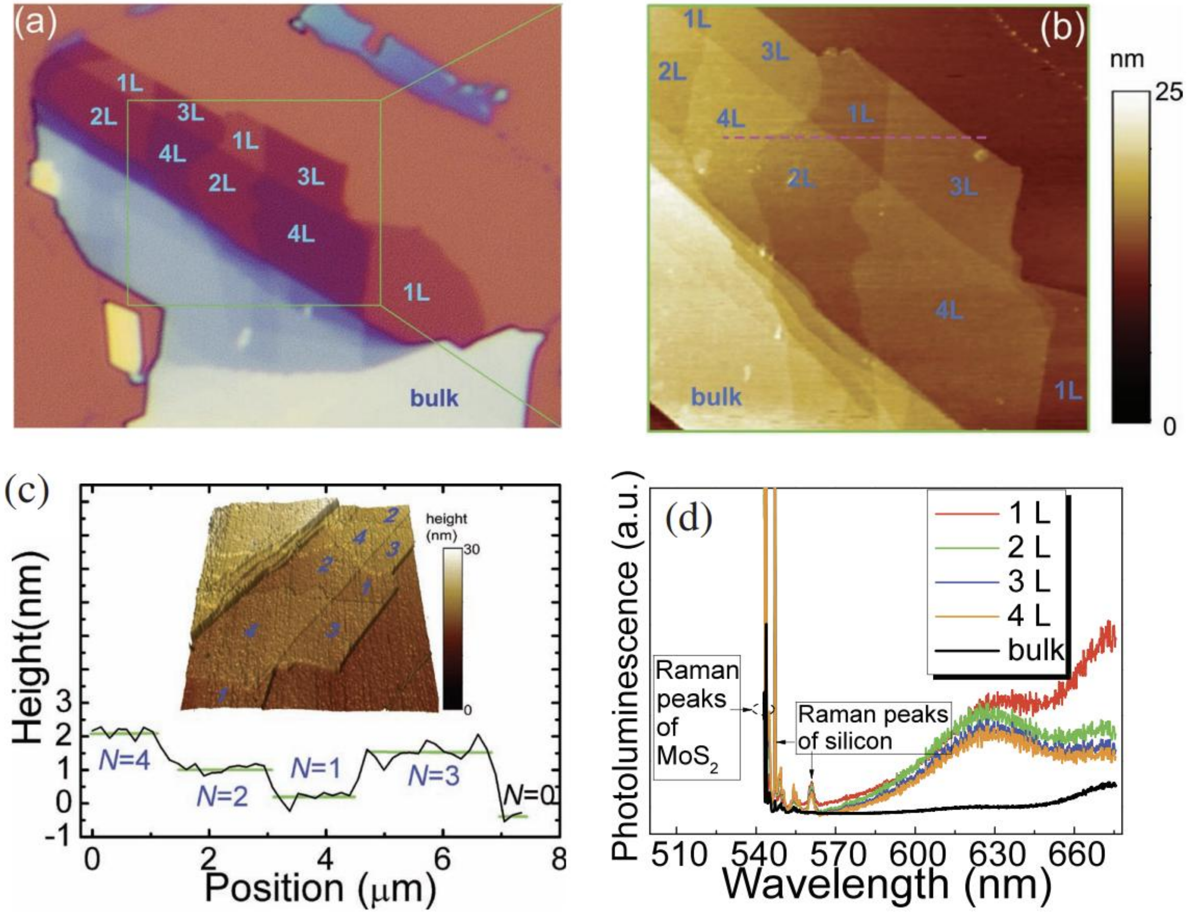

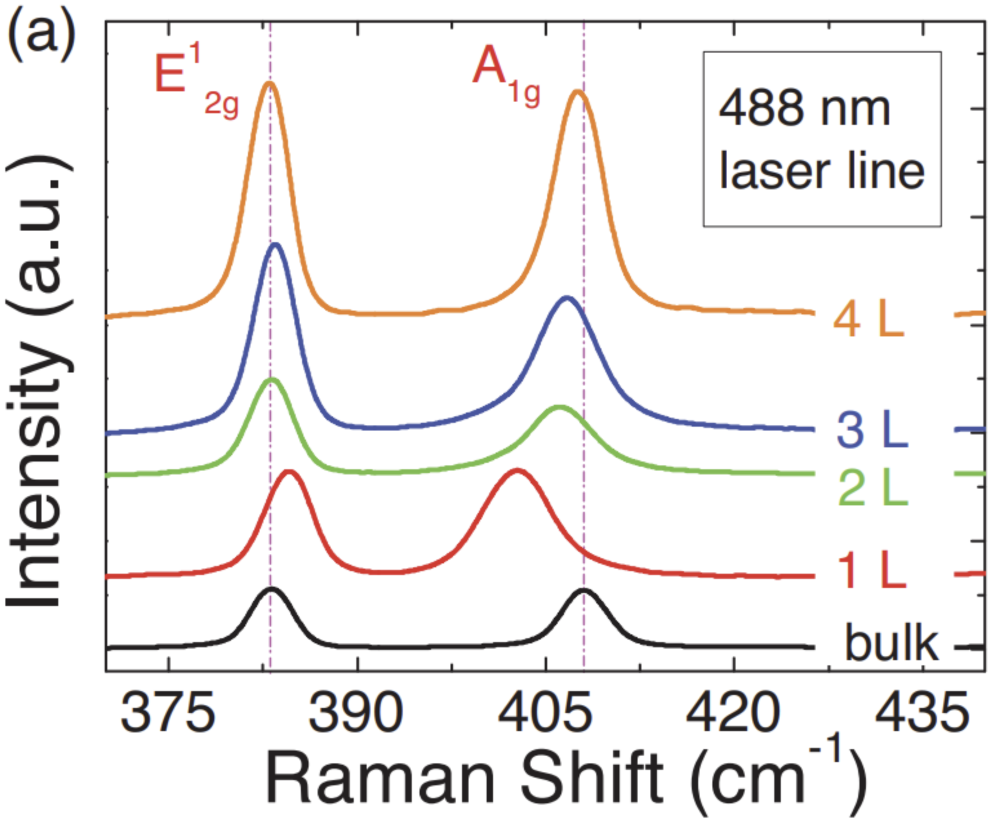

Adv. Ftn. Mater. **22**, 1385 (2012).

Photoluminescence (PL)

- The re-emission of light by interband luminescence after a direct gap semiconductor has been excited by a photon with energy greater than E_g.

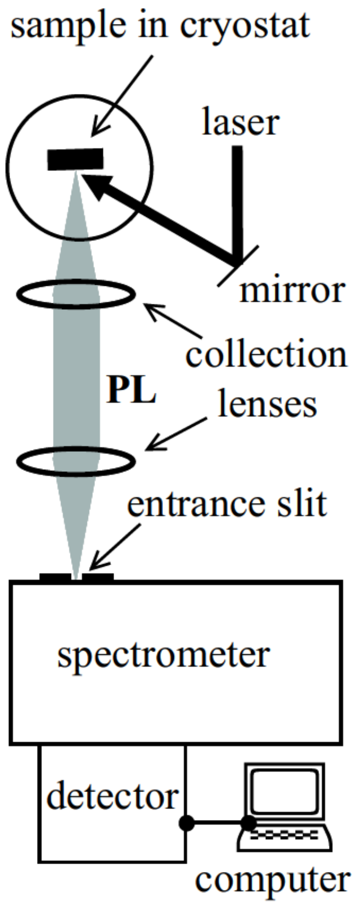

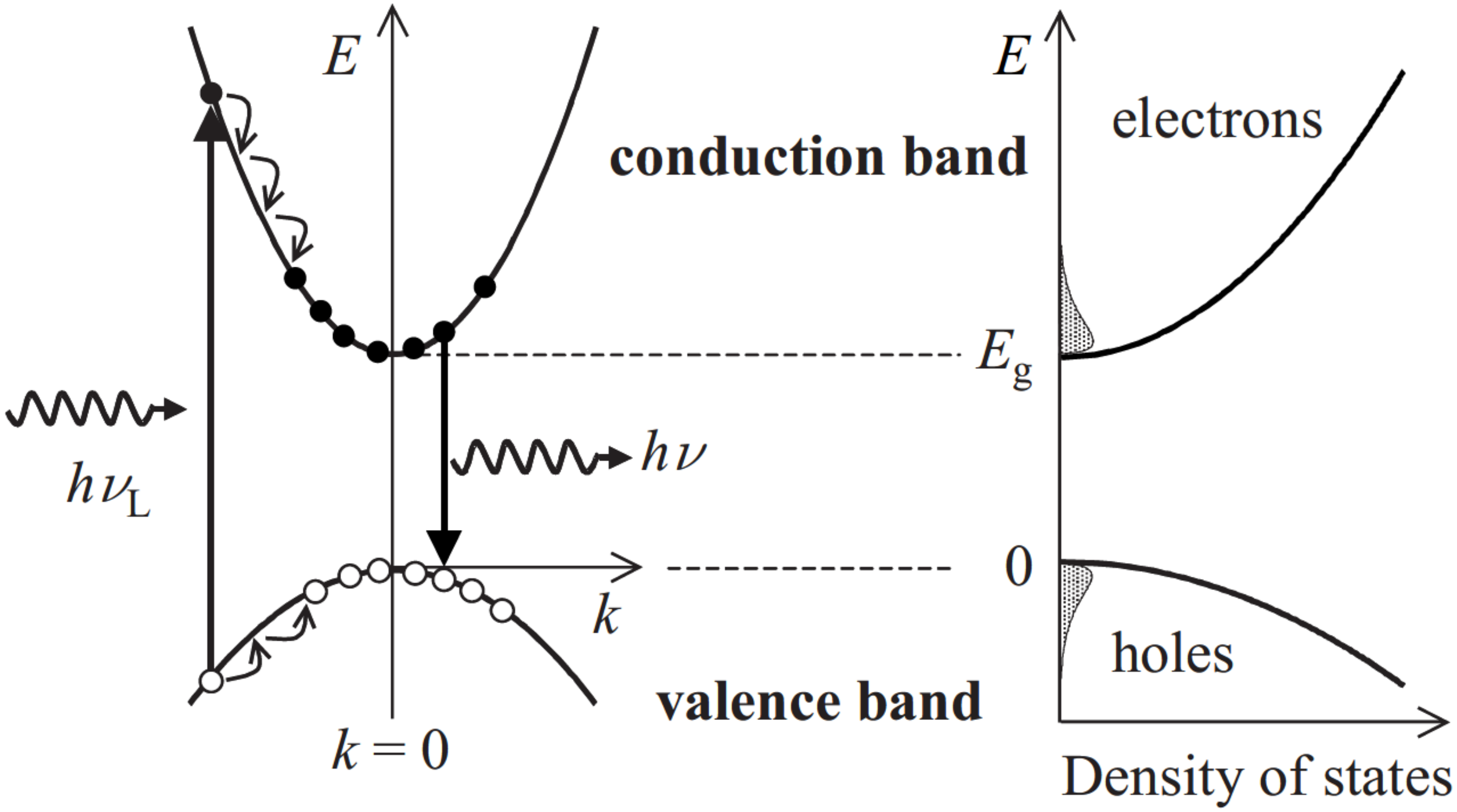

M. Fox, Optical properties of Solids, Oxford Univ. Press (2010)

Comparing the PL to the absorption

① Very thin/2D (mono~a few layer) sample:
- absorption very small (volume) + strong background (absorption from other transitions)
- PL measures emission from dark background ⟹ far superior SNR

② Distinguishes direct/indirect transition:
- absorption: observes the direct transition and the (phonon-assisted) indirect gap transition
- PL: Much efficient for the direct gap

③ PL has more prominent features of low-energy states:
- absorption: often difficult to observe trions (exciton + e/h), defect levels, and localized excitons

④ Non-equilibrium / final state info.
- PL: The emission reflects the relaxed **final** state after the excitation. (valley-spin info.)
- absorption: Reflects the initial state state (selection rule)

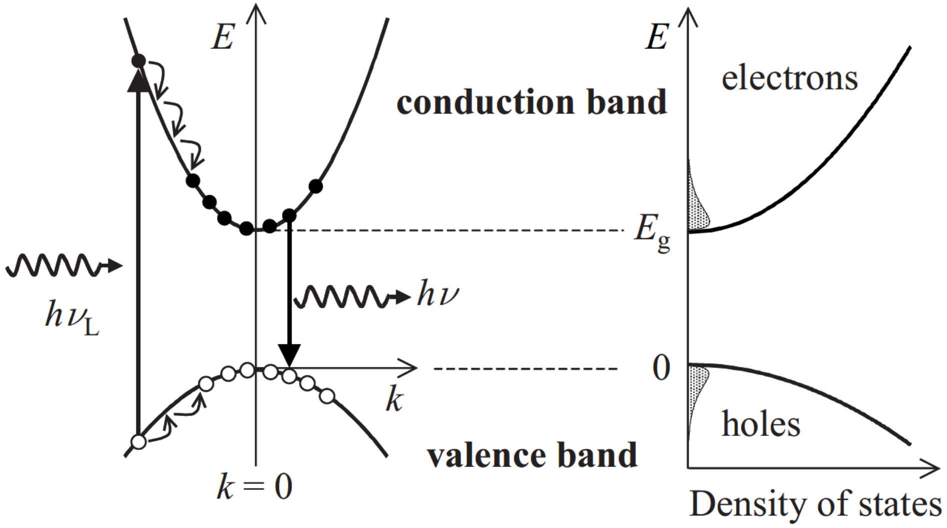

Indirect to direct band gap transition

PRL **105**, 136805 (2010) PHYSICAL REVIEW LETTERS week ending 24 SEPTEMBER 2010

Atomically Thin MoS_2: A New Direct-Gap Semiconductor

Kin Fai Mak,[1] Changgu Lee,[2] James Hone,[3] Jie Shan,[4] and Tony F. Heinz[1,*]

[1]*Departments of Physics and Electrical Engineering, Columbia University, 538 West 120th Street, New York, New York 10027, USA*

[2]*SKKU Advanced Institute of Nanotechnology (SAINT) and Department of Mechanical Engineering, Sungkyunkwan University, Suwon 440-746, Korea*

[3]*Department of Mechanical Engineering, Columbia University, New York, New York 10027, USA*

[4]*Department of Physics, Case Western Reserve University, 10900 Euclid Avenue, Cleveland, Ohio 44106, USA*

(Received 2 April 2010; published 24 September 2010)

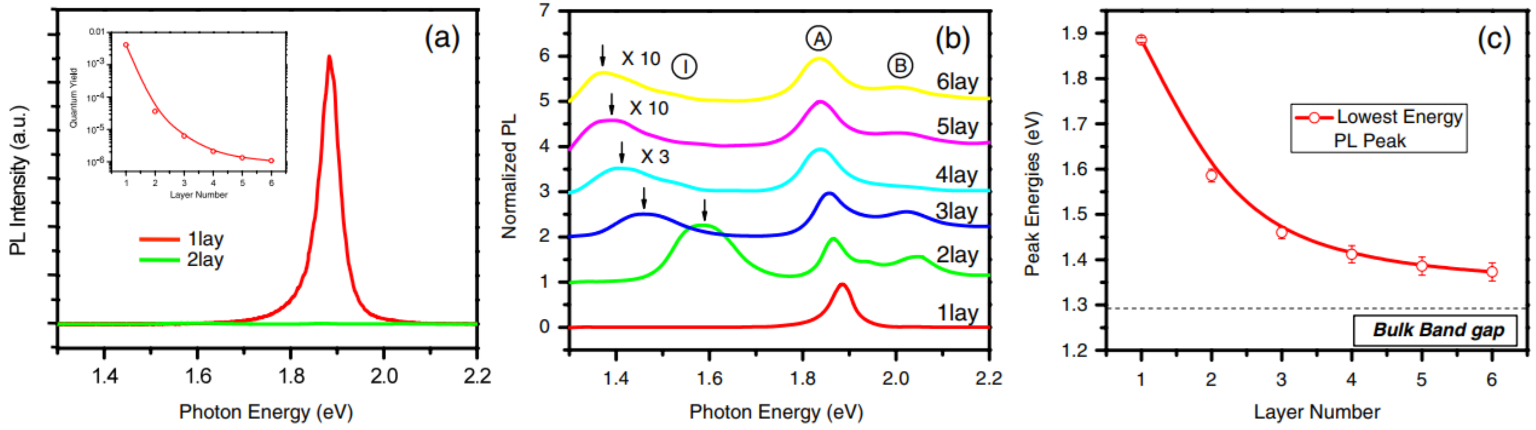

FIG. 3 (color online). (a) PL spectra for mono- and bilayer MoS_2 samples in the photon energy range from 1.3 to 2.2 eV. Inset: PL QY of thin layers for $N = 1$–6. (b) Normalized PL spectra by the intensity of peak A of thin layers of MoS_2 for $N = 1$–6. Feature I for $N = 4$–6 is magnified and the spectra are displaced for clarity. (c) Band-gap energy of thin layers of MoS_2, inferred from the energy of the PL feature I for $N = 2$–6 and from the energy of the PL peak A for $N = 1$. The dashed line represents the (indirect) band-gap energy of bulk MoS_2.

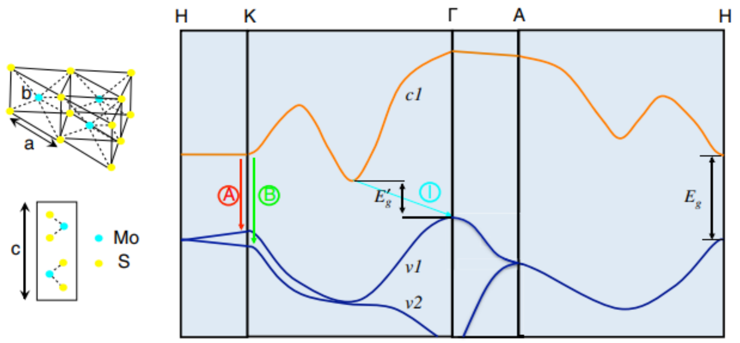

FIG. 1 (color online). Lattice structure of MoS_2 in both the in- and out-of-plane directions and simplified band structure of bulk MoS_2, showing the lowest conduction band $c1$ and the highest split valence bands $v1$ and $v2$. A and B are the direct-gap transitions, and I is the indirect-gap transition. E'_g is the indirect gap for the bulk, and E_g is the direct gap for the monolayer.

① MoS_2 undergoes indirect (bulk) to direct (monolayer) band gap transition with layer thickness.

② The PL intensity enhances significantly for direct band gap transition.

Exciton

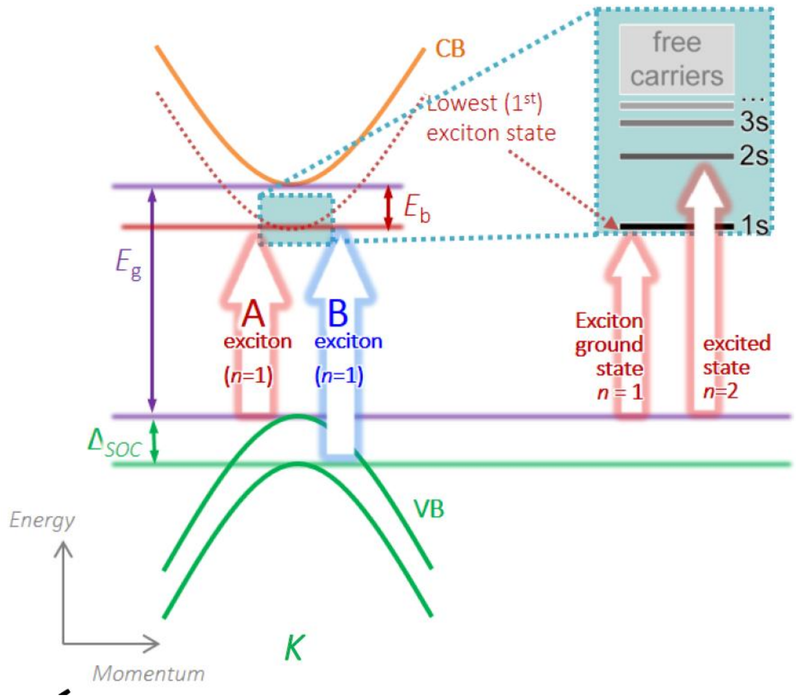

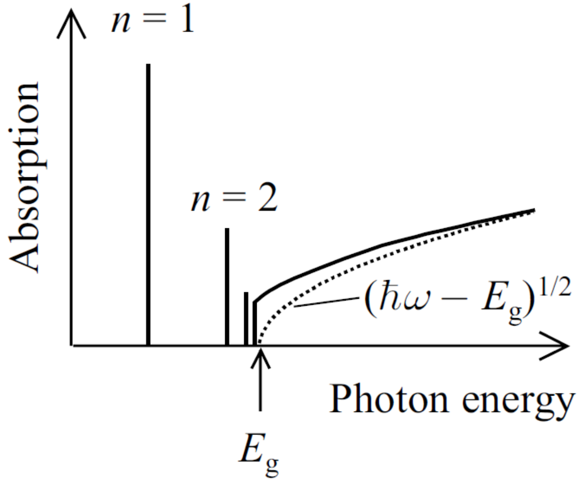

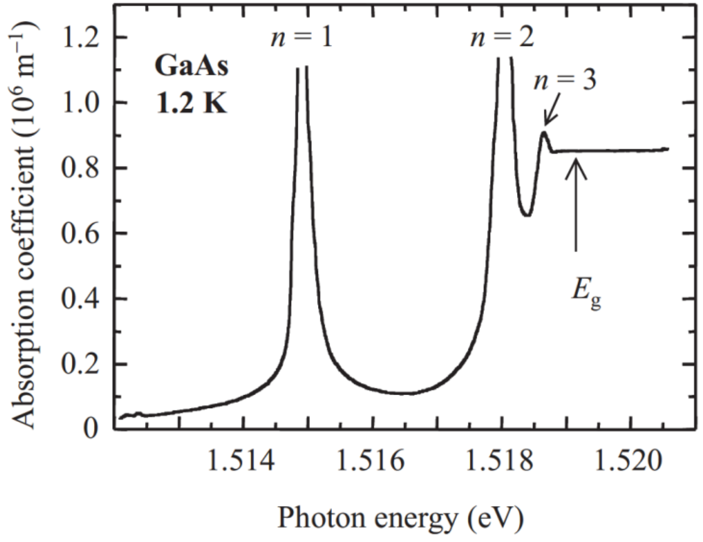

- The interband transition creates an electron in the CB and a hole in the VB.
- The oppositely charged particles are created at the same point in space and can attract each other through their mutual Coulomb interaction.
- The attractive interaction increases the probability of the formation of an electron-hole pair, and this neutral bound pair is called an exciton.
- Wannier-Mott exciton (free exciton) in semiconductors
- Frenkel excitons (tightly bound exciton) in molecular crystals and insulators

Exciton

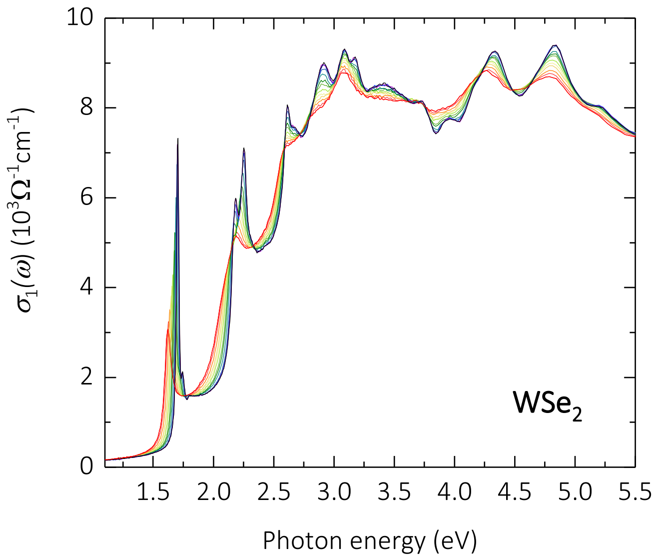

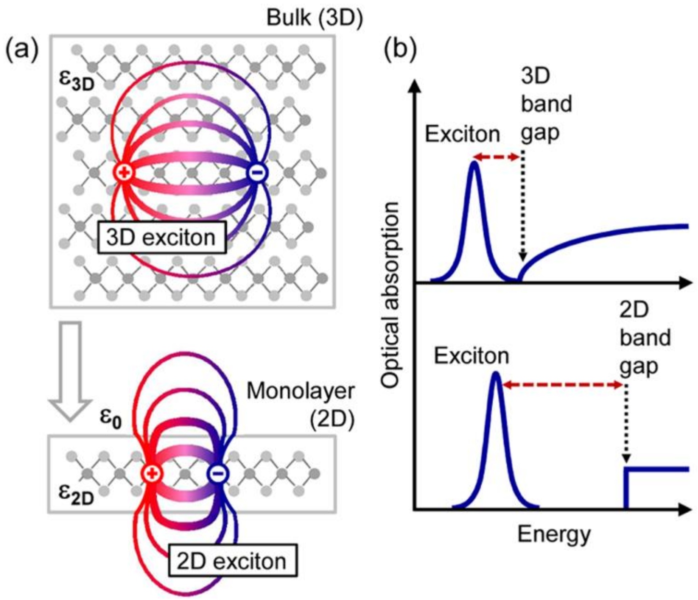

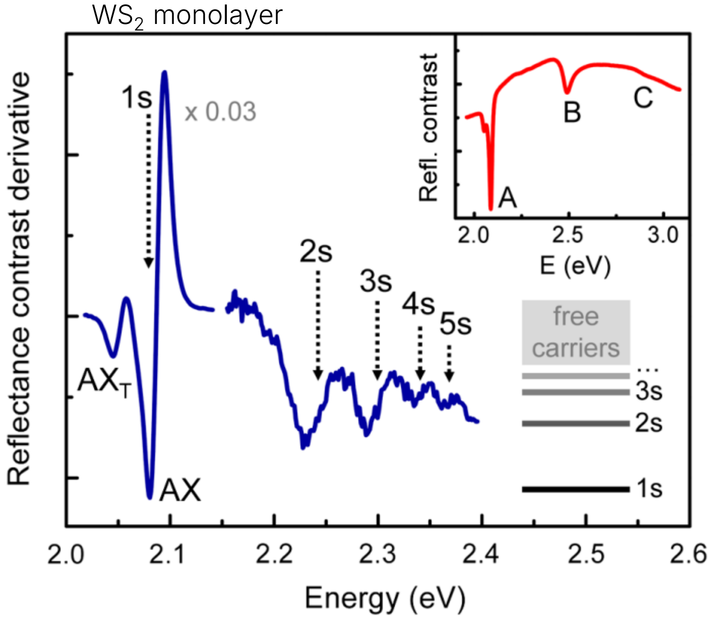

Heinz group, PRL **113**, 076802 (2014)

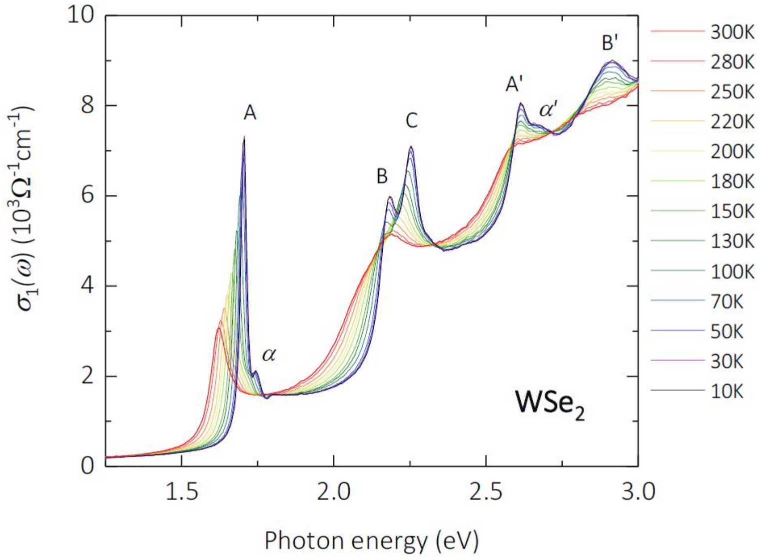

- Low dimensionality is advantageous to reduce the dielectric screening, which increases the electron-hole attraction and therefore the exciton binding energy.
- Research on strongly bound excitons in atomically thin semiconductors (TMDCs) — where **reduced dielectric screening** yields binding energies of hundreds of meV, making them stable even at room temperature — as a platform for exploring light–matter interactions, valley physics, and many-body phenomena, with applications toward next-generation optoelectronic devices.

Magnon

IR, one magnon

cf. THz spectroscopy

- Single ptl absorption; $\Delta q = 0$

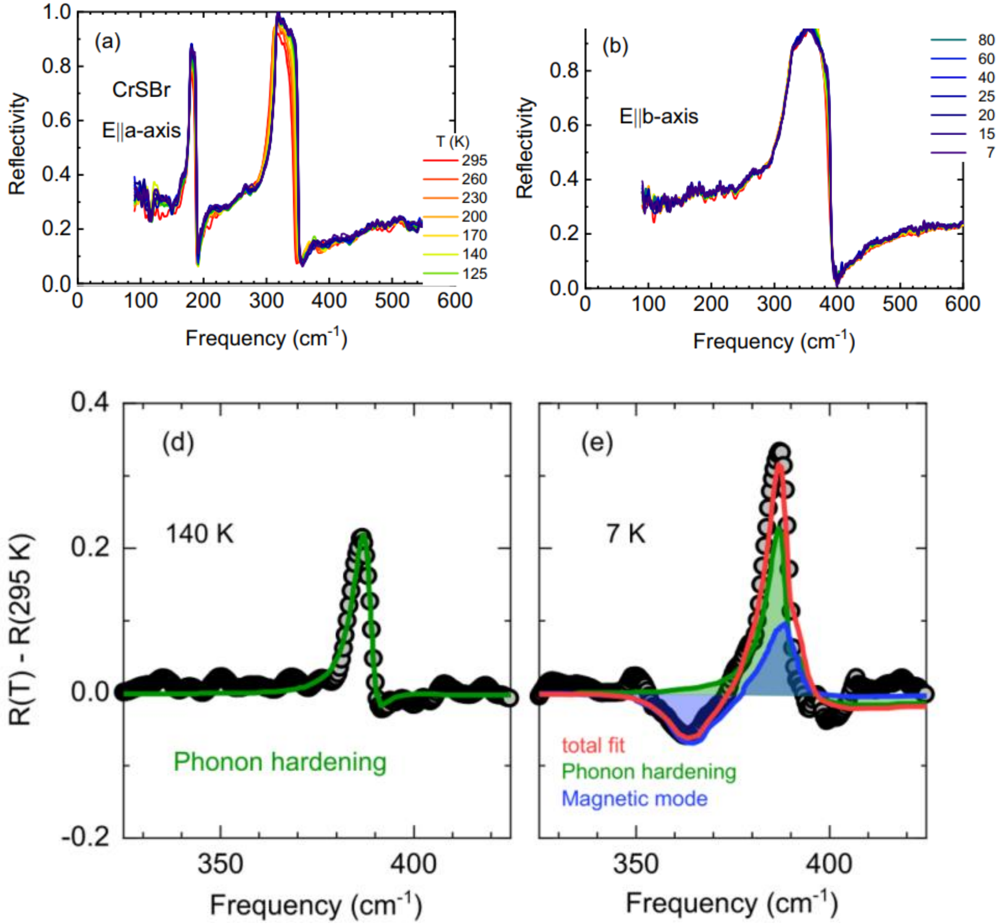

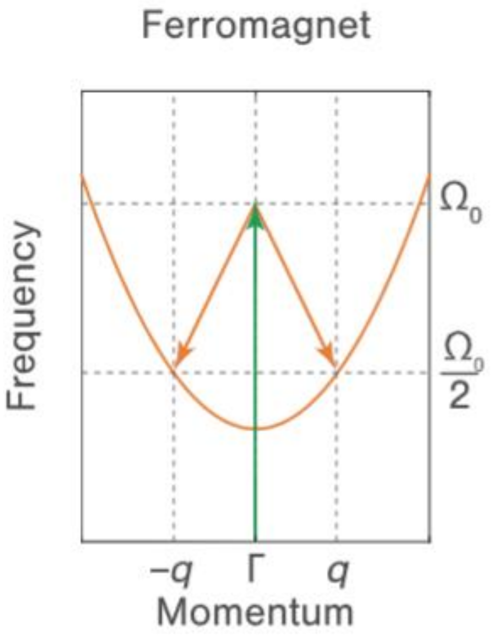

- Two ptl scattering;
  $\Delta q = 0 = +q + (-q)$

Sci. Adv. **11**, eadv3757 (2025)
Nat. Comm. **8**, 251 (2017)
Phys. Rev. **166**, 514 (1968)

Raman, two magnon

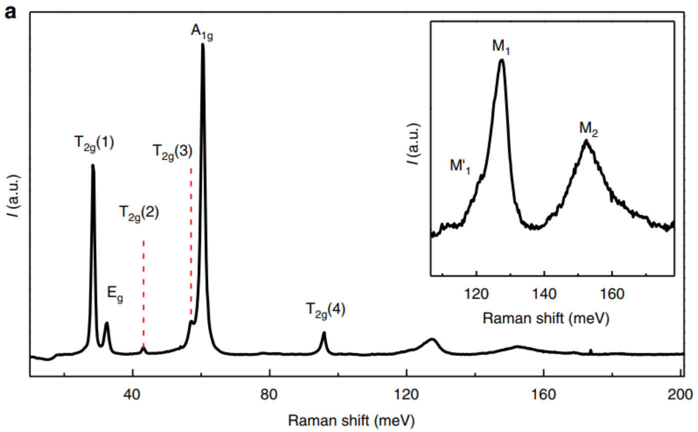

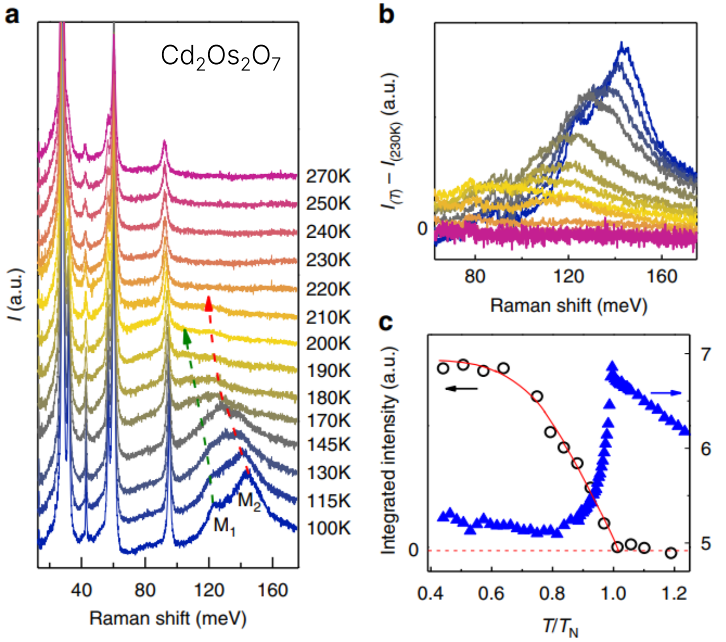

Universal scaling in free carrier regimes

Nature **425**, 271 (2003)

Quantum critical behaviour in a high-T_c superconductor

D. van der Marel[1]*, H. J. A. Molegraaf[1]*, J. Zaanen[2], Z. Nussinov[2]*, F. Carbone[1]*, A. Damascelli[3]*, H. Eisaki[3]*, M. Greven[3], P. H. Kes[2] & M. Li[2]

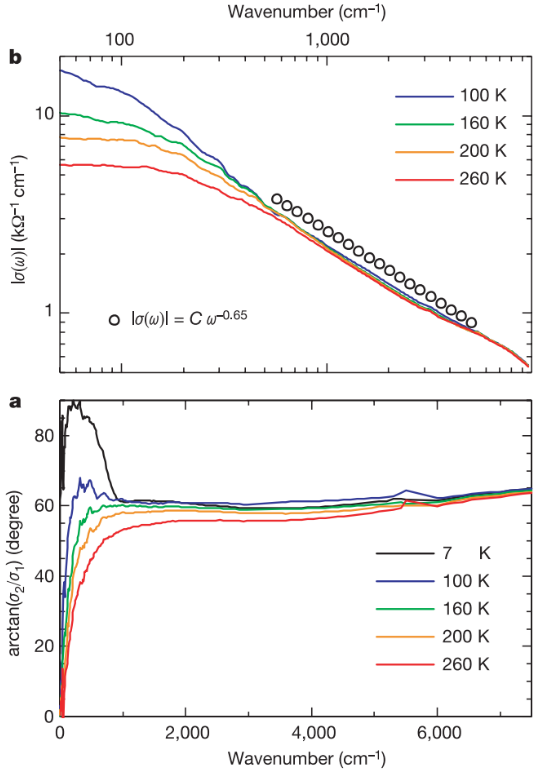

Nat. Comm. **14**, 3033 (2023)

nature communications

Article

https://doi.org/10.1038/s41467-023-38762-5

Reconciling scaling of the optical conductivity of cuprate superconductors with Planckian resistivity and specific heat

Received: 10 February 2023

Accepted: 11 May 2023

Published online: 26 May 2023

Bastien Michon[1,2,3], Christophe Berthod[1], Carl Willem Rischau[1], Amirreza Ataei[4], Lu Chen[4], Seiki Komiya[5], Shimpei Ono[5], Louis Taillefer[4,6], Dirk van der Marel[1] & Antoine Georges[1,7,8,9]

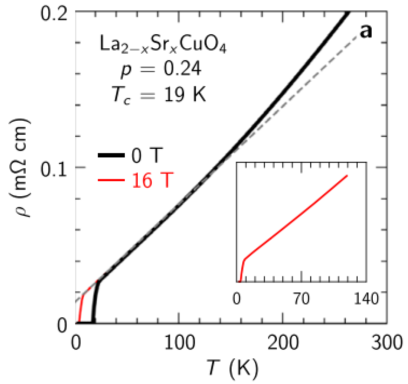

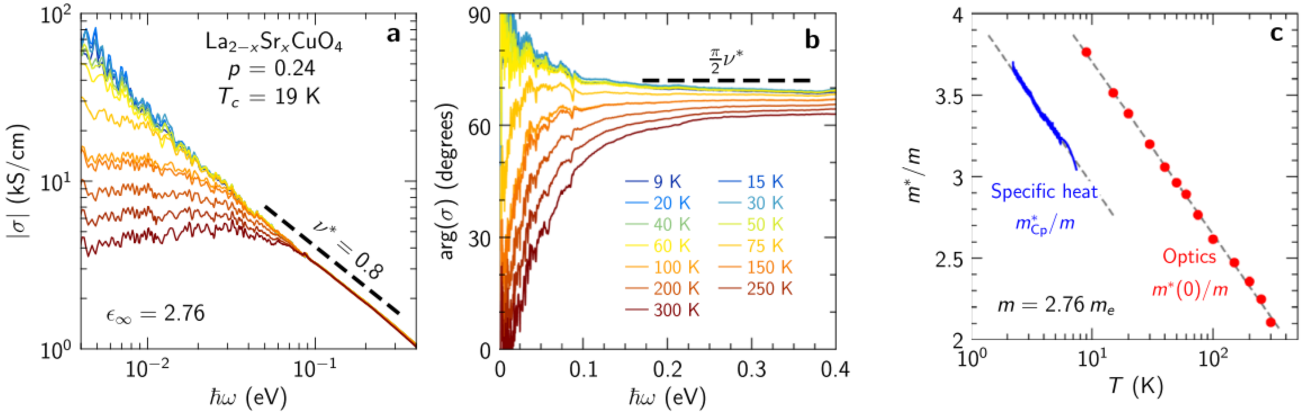

- Low energy $\sigma_1(\omega)$ scaling ($\sigma_1 \propto \omega^{-\alpha}$) provides information about the properties free carrier: Fermi liquid/Drude (α = 2), Plankian/bad metal (α = 1), quantum criticality(α < 1).

Contents

7/14 (화요일)

광분광학 (1)
이론 I: 평형상태 저에너지 분광학
- 광분광학의 기초
- 적외선 분광학

7/15 (수요일)

광분광학 (2)
- 엘립소미터
- Photoluminescence
- 라만 분광학

연구 적용 및 예시 I

7/20 (월요일)

광분광학 (3)
이론 II: 비평형상태 초고속 분광학
- 펌프-프루브 분광학
- tr-ARPES, tr-XRD

연구 적용 및 예시 II